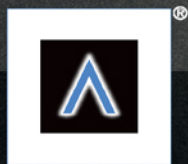
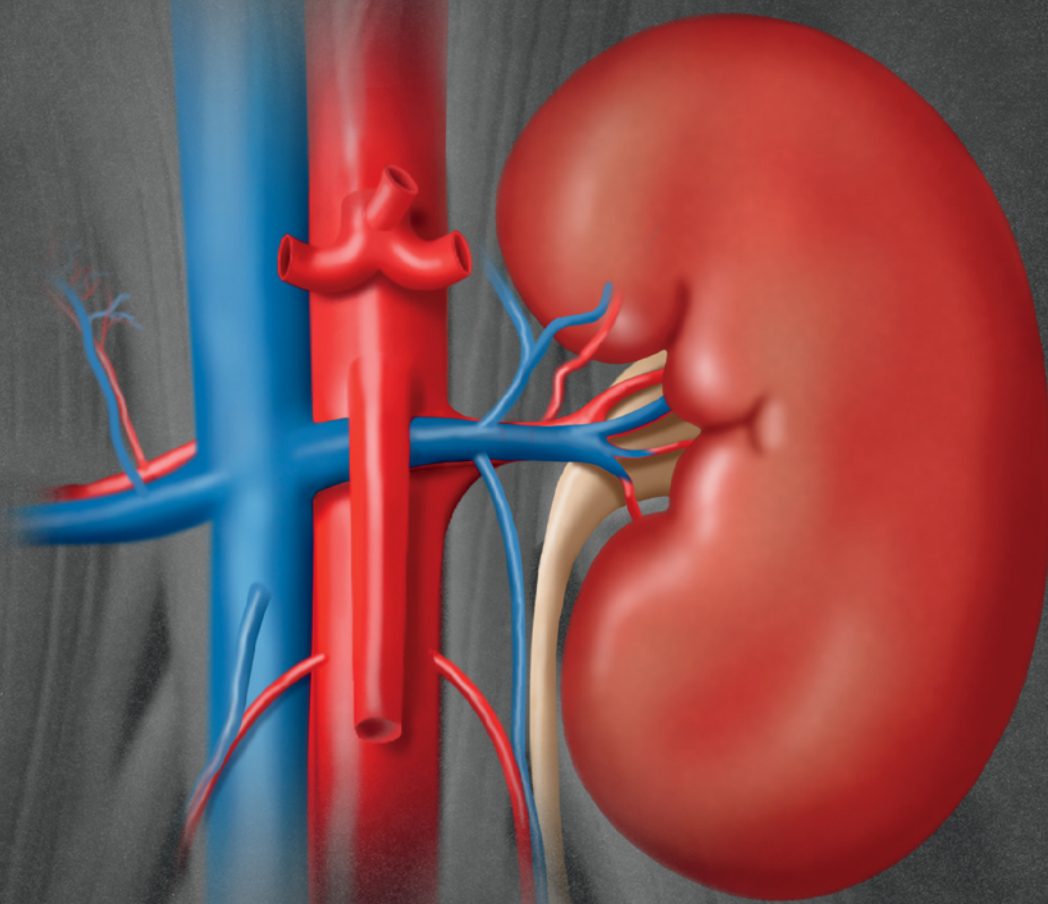


Get Full Access and More at

ExpertConsult.com

Diagnostic Imaging
Genitourinary

THIRD EDITION

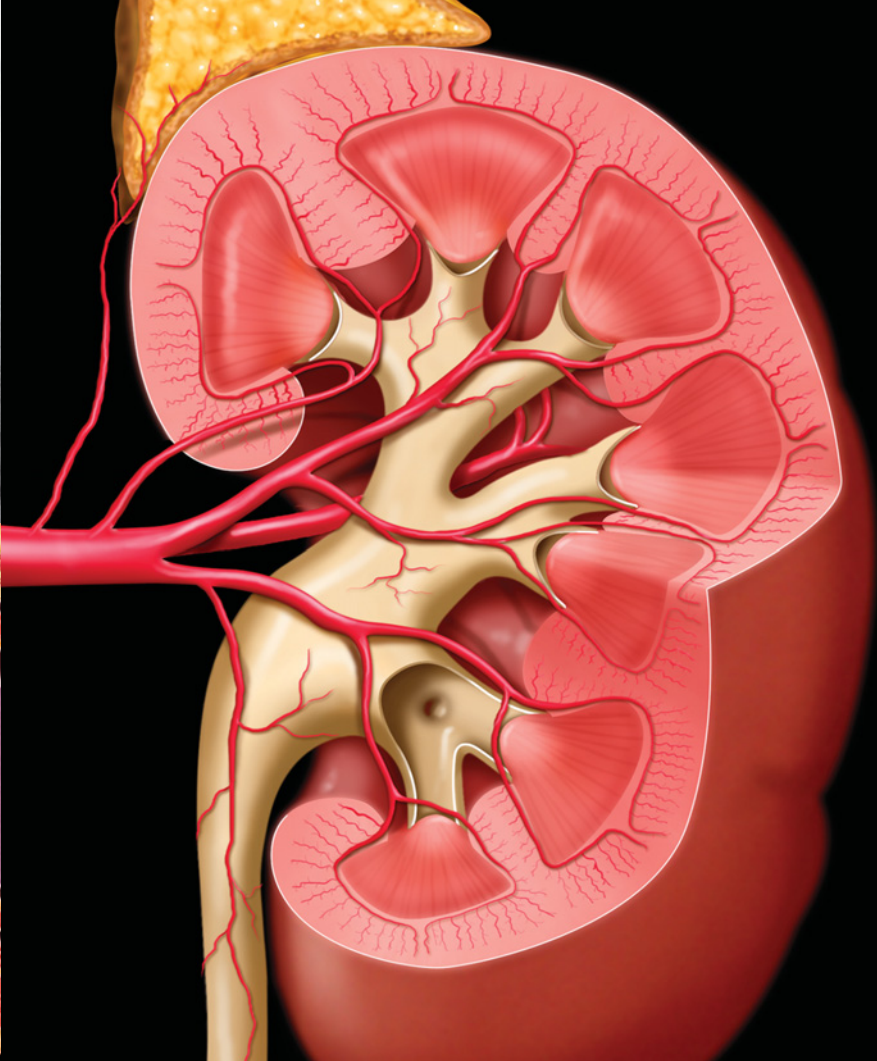
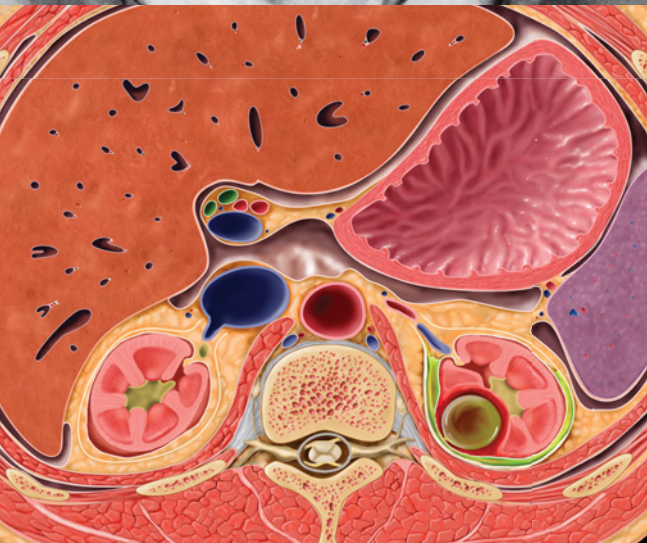
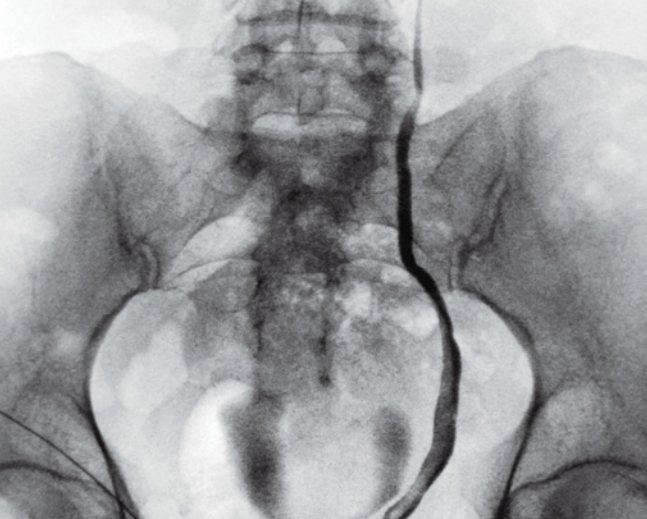


AMIRSYS®

ELSEVIER

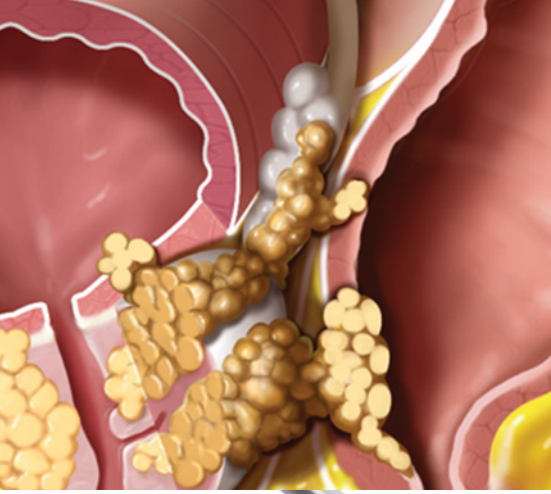
Tublin

BORHANI • FURLAN • HELLER



Diagnostic Imaging
Genitourinary

THIRD EDITION



Diagnostic Imaging

Genitourinary

THIRD EDITION

Mitchell Tublin, MD

Professor and Vice Chair of Radiology
Chief, Abdominal Imaging Division
University of Pittsburgh School of Medicine
Pittsburgh, Pennsylvania

Amir A. Borhani, MD

Assistant Professor of Radiology
Abdominal Imaging Division
University of Pittsburgh School of Medicine
Pittsburgh, Pennsylvania

Alessandro Furlan, MD

Assistant Professor
Abdominal Imaging Division
Department of Radiology
University of Pittsburgh School of Medicine
Pittsburgh, Pennsylvania

Matthew T. Heller, MD, FSAR

Associate Professor of Radiology
Abdominal Imaging Division
University of Pittsburgh Medical Center
Pittsburgh, Pennsylvania

Copyright © 2016 by Elsevier. All rights reserved.

No part of this publication may be reproduced or transmitted in any form or by any means, electronic or mechanical, including photocopying, recording, or any information storage and retrieval system, without permission in writing from the publisher. Details on how to seek permission, further information about the Publisher's permissions policies and our arrangements with organizations such as the Copyright Clearance Center and the Copyright Licensing Agency, can be found at our website: www.elsevier.com/permissions.

This book and the individual contributions contained in it are protected under copyright by the Publisher (other than as may be noted herein).

Notices

Knowledge and best practice in this field are constantly changing. As new research and experience broaden our understanding, changes in research methods, professional practices, or medical treatment may become necessary.

Practitioners and researchers must always rely on their own experience and knowledge in evaluating and using any information, methods, compounds, or experiments described herein. In using such information or methods they should be mindful of their own safety and the safety of others, including parties for whom they have a professional responsibility.

With respect to any drug or pharmaceutical products identified, readers are advised to check the most current information provided (i) on procedures featured or (ii) by the manufacturer of each product to be administered, to verify the recommended dose or formula, the method and duration of administration, and contraindications. It is the responsibility of practitioners, relying on their own experience and knowledge of their patients, to make diagnoses, to determine dosages and the best treatment for each individual patient, and to take all appropriate safety precautions.

To the fullest extent of the law, neither the Publisher nor the authors, contributors, or editors, assume any liability for any injury and/or damage to persons or property as a matter of products liability, negligence or otherwise, or from any use or operation of any methods, products, instructions, or ideas contained in the material herein.

Publisher Cataloging-in-Publication Data

Diagnostic imaging. Genitourinary / [edited by] Mitchell Tublin.
pages ; cm
Genitourinary
Includes bibliographical references and index.
ISBN 978-0-323-37708-9 (hardback)
1. Genitourinary organs--Cancer--Imaging--Handbooks, manuals, etc.
I. Tublin, Mitchell E. II. Title: Genitourinary.
[DNLN: 1. Urogenital Neoplasms--diagnosis--Atlases. 2. Diagnostic Imaging--Atlases. WJ 17]
RC280.G4 D534 2015
616.99/46--dc23

International Standard Book Number: 978-0-323-37708-9

Cover Designer: Tom M. Olson, BA
Cover Art: Lane R. Bennion, MS & Richard Coombs, MS
Printed in Canada by Friesens, Altona, Manitoba, Canada

Last digit is the print number: 9 8 7 6 5 4 3 2 1



Dedications

To the home team: My wonderful wife, Mary, and our sons, Daniel, Josh, and Andrew. The Tublin mantra: Good things happen with drive, commitment, and integrity...but it's really your love and support that make everything possible.

MT

I would like to dedicate this book to my wonderful wife, Goli, and to my beloved parents who have supported me in every second of my life.

AB

To Liz, for her patience, support, and love.

AF

*To Chiara, Sofia, and Oscar for their unwavering love and support.
To my mentor, Mitch Tublin, and my AI colleagues.
To my parents, Michelene and Tom.*

MH

Contributing Authors

Shweta Bhatt, MD

Associate Professor
Department of Imaging Sciences
University of Rochester Medical Center
Rochester, New York

Paula J. Woodward, MD

David G. Bragg, MD and Marcia R. Bragg
Presidential Endowed Chair in Oncologic
Imaging
Department of Radiology
Department of Obstetrics and Gynecology
University of Utah School of Medicine
Salt Lake City, Utah

Michael P. Federle, MD, FACR

Professor and Associate Chair for Education
Department of Radiology
Stanford University Medical Center
Stanford, California

R. Brooke Jeffrey, MD

Professor and Vice Chairman
Department of Radiology
Stanford University School of Medicine
Stanford, California

T. Gregory Walker, MD, FSIR

Assistant Professor of Radiology
Harvard Medical School
Associate Director, Fellowship
Division of Interventional Radiology
Massachusetts General Hospital
Boston, Massachusetts

Marta Heilbrun, MD, MS

Associate Professor of Radiology and Body
Imaging
University of Utah School of Medicine
Salt Lake City, Utah

Ashraf Thabet, MD

Instructor in Radiology
Harvard Medical School
Division of Interventional Radiology
Massachusetts General Hospital
Boston, Massachusetts

Gloria M. Salazar, MD

Assistant Radiologist
Division of Vascular Imaging and Intervention
Massachusetts General Hospital
Instructor in Radiology
Harvard Medical School
Boston, Massachusetts

Todd M. Blodgett, MD

Foundation Radiology Group
Pittsburgh, Pennsylvania

Katherine E. Maturen, MD, MS

Associate Professor
Abdominal Radiology Fellowship Director
University of Michigan Hospitals
Ann Arbor, Michigan

David Bauer, MD

Missoula Radiology
Missoula, Montana



Akram M. Shaaban, MBBCh

Professor (Clinical)
Department of Radiology
University of Utah School of Medicine
Salt Lake City, Utah

Christine O. Menias, MD

Professor of Radiology
Mayo Clinic School of Medicine
Scottsdale, Arizona
Adjunct Professor of Radiology
Washington University School of Medicine
St. Louis, Missouri

Vineet Krishan Khanna, MD

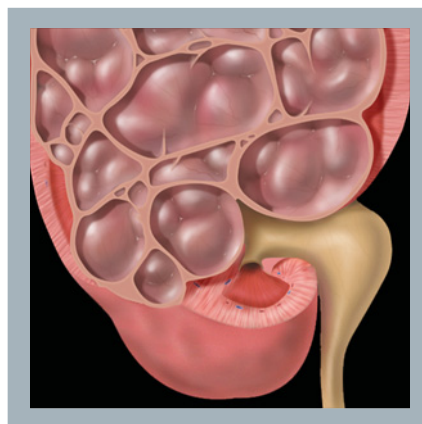
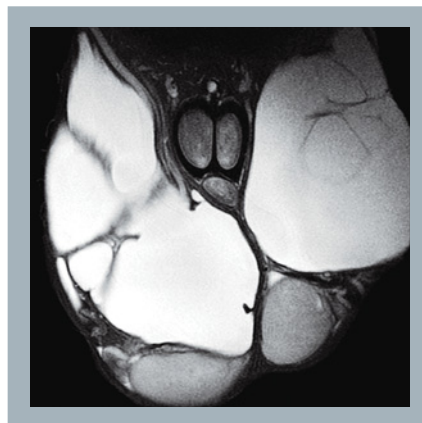
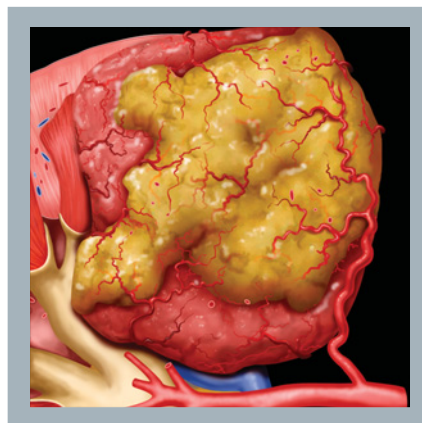
Radiology Resident
Department of Radiology
University of Pittsburgh Medical Center
Pittsburgh, Pennsylvania

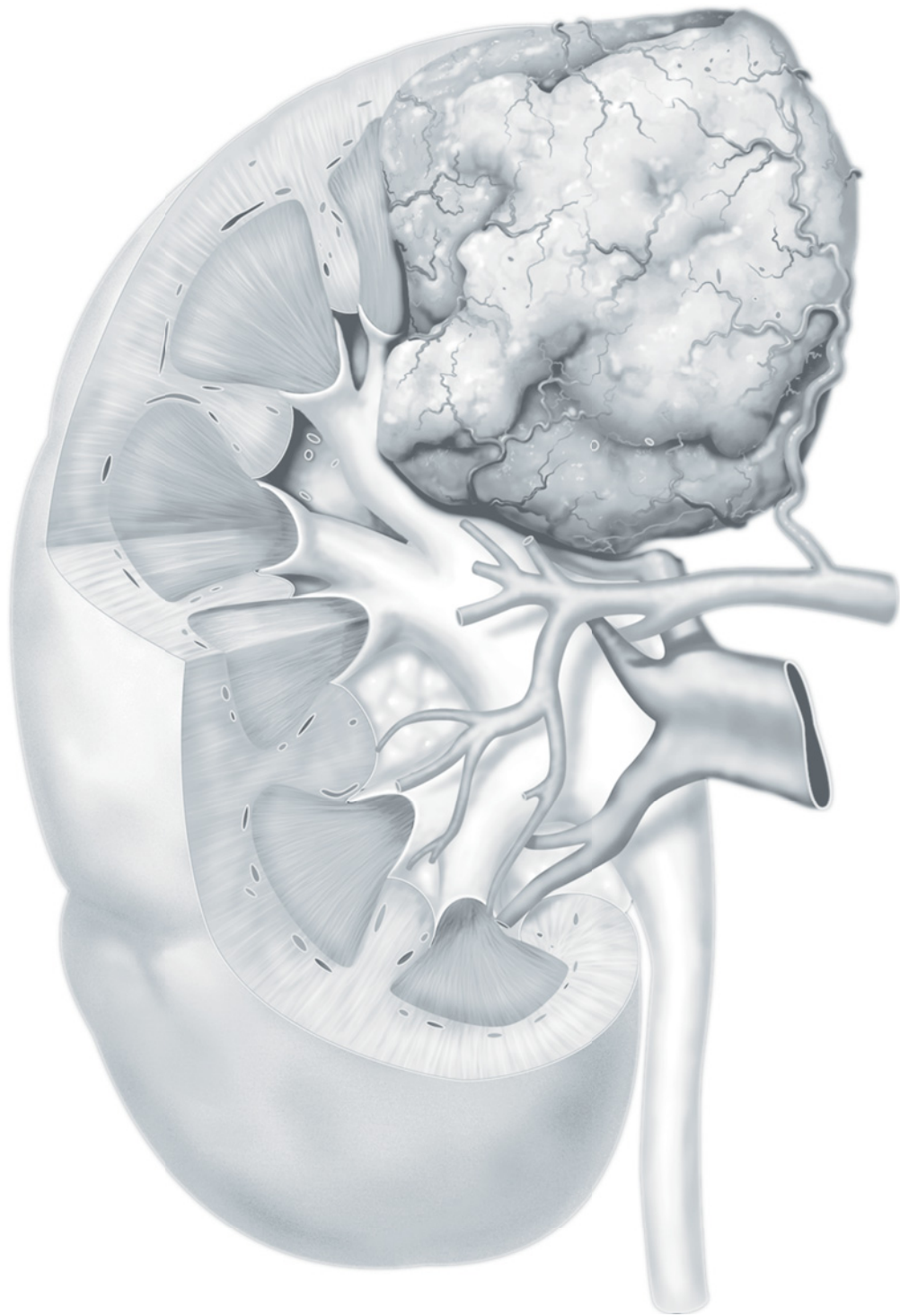
Karl Yaeger, MD

Women's Imaging Fellow
Department of Radiology
Magee Women's Hospital of UPMC
Pittsburgh, Pennsylvania

Amit B. Desai, MD

Radiology Resident
Department of Imaging Sciences
University of Rochester Medical Center
Rochester, New York





Preface

Abdominal imagers recognize that a formal rigid split between GU and GI radiology no longer works with the rapid advancements in cross-sectional imaging that have occurred over the past generation. Nonetheless, when we began planning for the third edition of *Diagnostic Imaging: Abdomen*, we realized that it was no longer possible to encompass the imaging and management of the entire spectrum of abdominal disorders in one text. Thus we decided to separate diagnoses considered to be largely genitourinary (highlighted in this updated and expanded text) from topics judged to be gastrointestinal (covered in a corresponding, companion book).

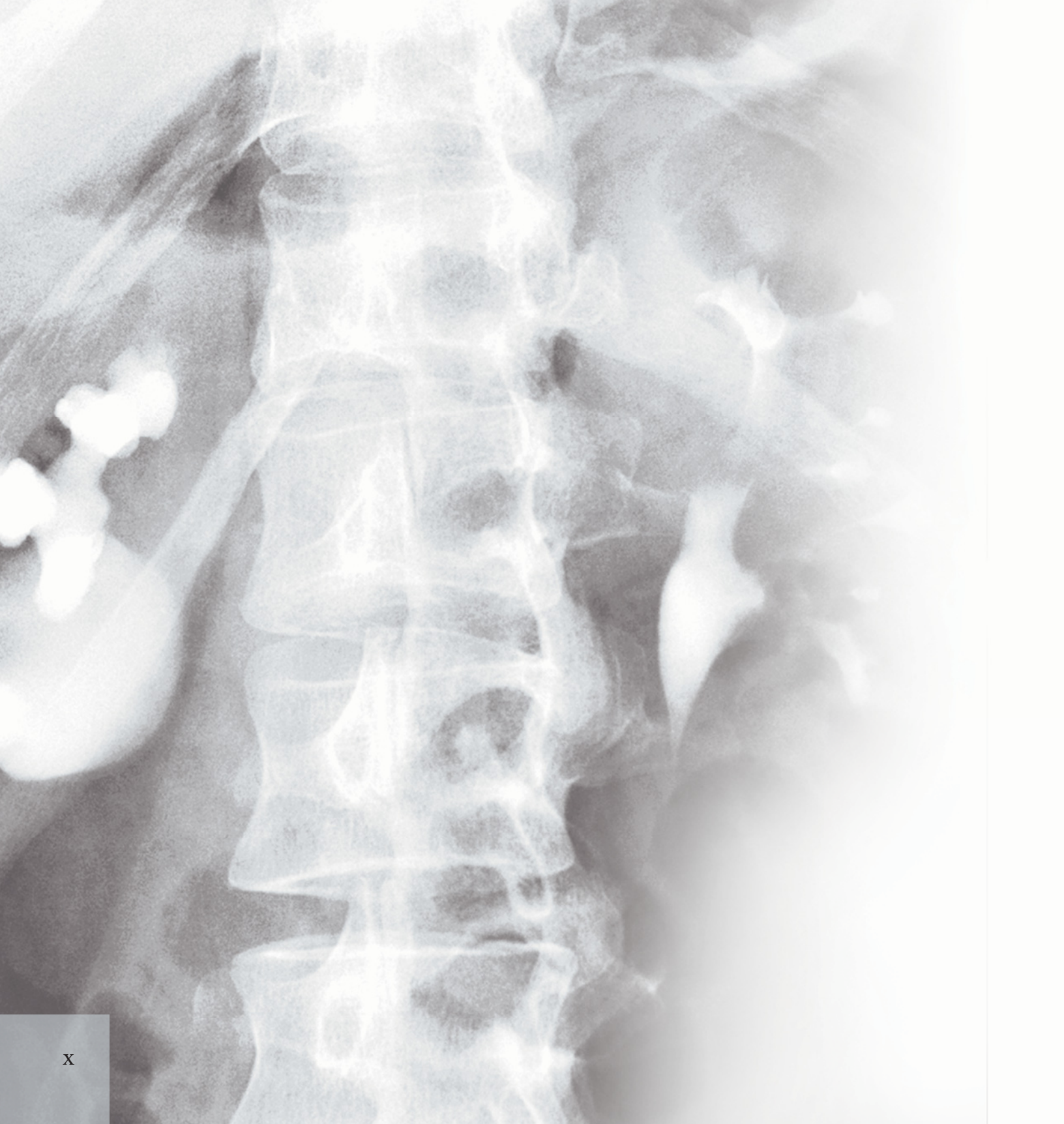
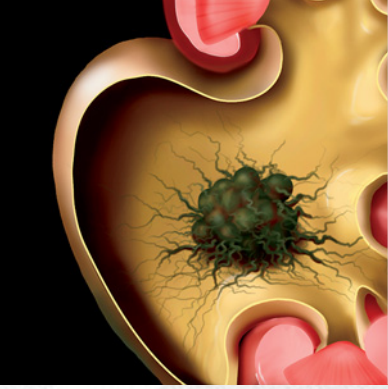
The Amirsys format of bulleted text — including key facts, imaging features, exam protocols, pathology, clinical manifestations/treatment, and image interpretation pearls — is still employed. Succinct but exhaustive outlined descriptions of GU diagnoses are supplemented by image galleries that emphasize the pearls and pitfalls of modern GU imaging. The number of genitourinary diagnoses has been significantly expanded, and the utility of state of the art cross-sectional imaging is emphasized in updated image panels. The approach mirrors current practice: Examples of traditional imaging techniques utilized by GU radiologists decades ago (retrograde, intravenous urography, angiography, etc.) have largely been replaced by their cross-sectional counterparts (MDCT, MR, CTA, MRA, CT urography, MR urography)

employed by present day abdominal imagers. Introductory narrative overview chapters describe relevant GU anatomy, physiology, imaging protocols and work-up. GU oncology staging and interventional technique chapters — crucial material for current abdominal imagers — have also been added. Finally, additional images and references are included in the Elsevier Expert Consult eBook that accompanies the print version of *Diagnostic Imaging: Genitourinary, Third Edition*.

This new edition of *Diagnostic Imaging: Genitourinary* was compiled by members of the Abdominal Imaging Division of the University of Pittsburgh. The division has a long history of excellent collaboration with one another, and with referring clinical services. This collaboration has resulted in a legacy of clinical and academic success, and will be even more important in a healthcare environment that appropriately emphasizes value over volume. We are confident that this updated edition will be a go-to, readily accessible, clinically relevant resource for abdominal imagers and trainees for years to come.

Mitchell Tublin, MD

Professor and Vice Chair of Radiology
Chief, Abdominal Imaging Division
University of Pittsburgh School of Medicine
Pittsburgh, Pennsylvania



Acknowledgements

Text Editors

Dave L. Chance, MA, ELS
Arthur G. Gelsinger, MA
Nina I. Bennett, BA
Sarah J. Connor, BA
Tricia L. Cannon, BA
Terry W. Ferrell, MS
Lisa A. Gervais, BS
Karen E. Concannon, MA, PhD

Image Editors

Jeffrey J. Marmorstone, BS
Lisa A. M. Steadman, BS

Medical Editor

Anil K. Dasyam, MD

Illustrations

Richard Coombs, MS
Lane R. Bennion, MS
Laura C. Sesto, MA

Art Direction and Design

Tom M. Olson, BA
Laura C. Sesto, MA

Lead Editor

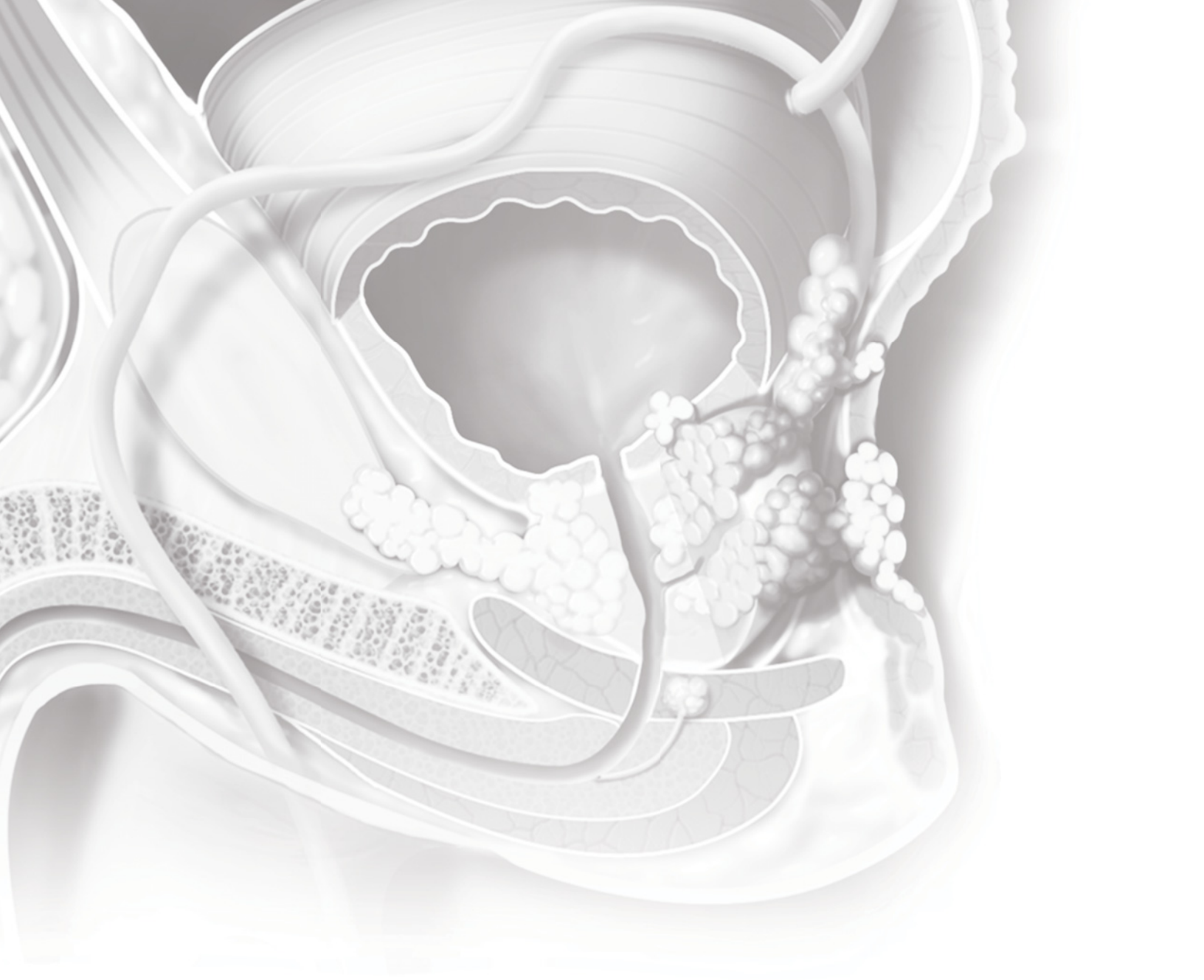
Tricia L. Cannon, BA

Production Coordinators

Rebecca L. Hutchinson, BA
Angela M.G. Terry, BA

ELSEVIER





Sections

SECTION 1: OVERVIEW AND INTRODUCTION

SECTION 2: RETROPERITONEUM

SECTION 3: ADRENAL

SECTION 4: KIDNEY AND RENAL PELVIS

SECTION 5: URETER

SECTION 6: BLADDER

SECTION 7: URETHRA/PENIS

SECTION 8: TESTES

SECTION 9: EPIDIDYMIS

SECTION 10: SCROTUM

SECTION 11: SEMINAL VESICLES

SECTION 12: PROSTATE

SECTION 13: PROCEDURES

TABLE OF CONTENTS

SECTION 1: OVERVIEW AND INTRODUCTION

- 4 **Imaging Approaches**
Mitchell Tublin, MD

SECTION 2: RETROPERITONEUM

- 12 **Introduction to the Retroperitoneum**
Matthew T. Heller, MD, FSAR

CONGENITAL

- 16 **Duplications and Anomalies of IVC**
Matthew T. Heller, MD, FSAR

INFLAMMATION

- 20 **Retroperitoneal Fibrosis**
Matthew T. Heller, MD, FSAR

DEGENERATIVE

- 24 **Pelvic Lipomatosis**
Matthew T. Heller, MD, FSAR

TREATMENT RELATED

- 26 **Coagulopathic (Retroperitoneal) Hemorrhage**
Matthew T. Heller, MD, FSAR
- 30 **Postoperative Lymphocele**
Matthew T. Heller, MD, FSAR

BENIGN NEOPLASMS

- 32 **Retroperitoneal Neurogenic Tumor**
Matthew T. Heller, MD, FSAR

MALIGNANT NEOPLASMS

- 36 **Retroperitoneal Sarcoma**
Matthew T. Heller, MD, FSAR and Michael P. Federle, MD, FACR
- 40 **Retroperitoneal and Mesenteric Lymphoma**
Matthew T. Heller, MD, FSAR
- 44 **Retroperitoneal Metastases**
Matthew T. Heller, MD, FSAR
- 48 **Hemangiopericytoma**
Matthew T. Heller, MD, FSAR
- 50 **Perivascular Epithelioid Cell Tumor (PEComa)**
Matthew T. Heller, MD, FSAR

SECTION 3: ADRENAL

- 54 **Introduction to the Adrenals**
Mitchell Tublin, MD and Michael P. Federle, MD, FACR

INFECTION

- 58 **Adrenal Tuberculosis and Fungal Infection**
Mitchell Tublin, MD and Michael P. Federle, MD, FACR

METABOLIC OR INHERITED

- 60 **Adrenal Hyperplasia**
Mitchell Tublin, MD and Michael P. Federle, MD, FACR
- 64 **Adrenal Insufficiency**
Mitchell Tublin, MD and Michael P. Federle, MD, FACR

TRAUMA

- 66 **Adrenal Hemorrhage**
Mitchell Tublin, MD and Michael P. Federle, MD, FACR

BENIGN NEOPLASMS

- 70 **Adrenal Cyst**
Mitchell Tublin, MD
- 74 **Adrenal Adenoma**
Mitchell Tublin, MD
- 80 **Adrenal Myelolipoma**
Mitchell Tublin, MD and Michael P. Federle, MD, FACR
- 84 **Pheochromocytoma**
Mitchell Tublin, MD

MALIGNANT NEOPLASMS

- 90 **Adrenal Carcinoma**
Mitchell Tublin, MD and Michael P. Federle, MD, FACR
- 94 **Adrenal Carcinoma Staging**
Marta Heilbrun, MD, MS
- 104 **Adrenal Lymphoma**
Mitchell Tublin, MD
- 106 **Adrenal Metastases**
Mitchell Tublin, MD
- 110 **Adrenal Collision Tumor**
Mitchell Tublin, MD and Michael P. Federle, MD, FACR

SECTION 4: KIDNEY AND RENAL PELVIS

- 114 **Introduction to Renal Physiology and Contrast**
Alessandro Furlan, MD
- 116 **Introduction to the Kidney and Renal Pelvis**
Alessandro Furlan, MD

NORMAL VARIANTS AND PSEUDOLESIONS

- 122 **Renal Fetal Lobation**
Amir A. Borhani, MD and Michael P. Federle, MD, FACR
- 124 **Junctional Cortical Defect**
Amir A. Borhani, MD

TABLE OF CONTENTS

- 126 **Column of Bertin**
Amir A. Borhani, MD and Michael P. Federle, MD, FACR

CONGENITAL

- 128 **Horseshoe Kidney**
Alessandro Furlan, MD and Michael P. Federle, MD, FACR
- 132 **Renal Ectopia and Agenesis**
Alessandro Furlan, MD and Michael P. Federle, MD, FACR
- 136 **Ureteropelvic Junction Obstruction**
Alessandro Furlan, MD and Michael P. Federle, MD, FACR
- 140 **Congenital Megacalyces and Megaureter**
Alessandro Furlan, MD
- 142 **Renal Lymphangiomatosis**
Alessandro Furlan, MD

INFECTION

- 144 **Acute Pyelonephritis**
Alessandro Furlan, MD
- 148 **Chronic Pyelonephritis/Reflux Nephropathy**
Alessandro Furlan, MD and Amir A. Borhani, MD
- 150 **Xanthogranulomatous Pyelonephritis**
Alessandro Furlan, MD and R. Brooke Jeffrey, MD
- 154 **Emphysematous Pyelonephritis**
Alessandro Furlan, MD and R. Brooke Jeffrey, MD
- 156 **Renal Abscess**
Alessandro Furlan, MD and R. Brooke Jeffrey, MD
- 160 **Pyonephrosis**
Alessandro Furlan, MD
- 162 **Opportunistic Renal Infections**
Alessandro Furlan, MD and Amir A. Borhani, MD

RENAL CYSTIC DISEASE

- 164 **Renal Cyst**
Alessandro Furlan, MD
- 168 **Parapelvic (Peripelvic) Cyst**
Alessandro Furlan, MD
- 170 **Autosomal Dominant Polycystic Kidney Disease**
Alessandro Furlan, MD
- 174 **Uremic Cystic Disease**
Alessandro Furlan, MD
- 176 **von Hippel-Lindau Disease**
Alessandro Furlan, MD
- 178 **Medullary Cystic Kidney Disease**
Michael P. Federle, MD, FACR
- 180 **Lithium Nephropathy**
Alessandro Furlan, MD and Amir A. Borhani, MD
- 182 **Localized Cystic Renal Disease**
Alessandro Furlan, MD and Michael P. Federle, MD, FACR

BENIGN NEOPLASMS

- 184 **Renal Angiomyolipoma**
Matthew T. Heller, MD, FSAR
- 190 **Renal Oncocytoma**
Matthew T. Heller, MD, FSAR
- 194 **Metanephric Adenoma**
Matthew T. Heller, MD, FSAR

- 196 **Multilocular Cystic Nephroma**
Matthew T. Heller, MD, FSAR and Michael P. Federle, MD, FACR

- 200 **Mixed Epithelial and Stromal Tumor**
Matthew T. Heller, MD, FSAR

MALIGNANT NEOPLASMS

- 202 **Renal Cell Carcinoma**
Matthew T. Heller, MD, FSAR
- 208 **Renal Cell Carcinoma Staging**
Todd M. Blodgett, MD and Karl Yaeger, MD and Vineet Krishan Khanna, MD
- 232 **Medullary Carcinoma**
Matthew T. Heller, MD, FSAR
- 234 **Collecting Duct Carcinoma**
Matthew T. Heller, MD, FSAR
- 236 **Renal Transitional Cell Carcinoma**
Matthew T. Heller, MD, FSAR
- 240 **Renal Pelvis and Ureteral Carcinoma Staging**
Akram M. Shaaban, MBBCh
- 256 **Renal Lymphoma**
Matthew T. Heller, MD, FSAR
- 258 **Renal Metastases**
Matthew T. Heller, MD, FSAR

METABOLIC

- 260 **Nephrocalcinosis**
Matthew T. Heller, MD, FSAR and Michael P. Federle, MD, FACR
- 264 **Urolithiasis**
Matthew T. Heller, MD, FSAR
- 268 **Paroxysmal Nocturnal Hemoglobinuria**
Matthew T. Heller, MD, FSAR

RENAL FAILURE AND MEDICAL RENAL DISEASE

- 270 **Hydronephrosis**
Alessandro Furlan, MD
- 272 **Glomerulonephritis**
Michael P. Federle, MD, FACR
- 274 **Acute Tubular Necrosis**
Alessandro Furlan, MD
- 276 **Renal Cortical Necrosis**
Alessandro Furlan, MD
- 278 **Renal Papillary Necrosis**
Michael P. Federle, MD, FACR
- 280 **HIV Nephropathy**
Alessandro Furlan, MD
- 282 **Chronic Renal Failure**
Alessandro Furlan, MD
- 284 **Renal Lipomatosis**
Alessandro Furlan, MD and Amir A. Borhani, MD

VASCULAR DISORDERS

- 286 **Renal Artery Stenosis**
Amir A. Borhani, MD
- 290 **Renal Infarction**
Amir A. Borhani, MD

TABLE OF CONTENTS

- 296 **Renal Vein Thrombosis**
Amir A. Borhani, MD

TRAUMA

- 300 **Renal Trauma**
Matthew T. Heller, MD, FSAR
- 304 **Urinoma**
Matthew T. Heller, MD, FSAR

TRANSPLANTATION

- 306 **Renal Transplantation**
Mitchell Tublin, MD

TREATMENT RELATED

- 312 **Postoperative State, Kidney**
Amir A. Borhani, MD
- 316 **Radiation Nephritis**
Amir A. Borhani, MD
- 318 **Contrast-Induced Nephropathy**
Amir A. Borhani, MD

SECTION 5: URETER

- 324 **Introduction to the Ureter**
Amir A. Borhani, MD and Paula J. Woodward, MD

CONGENITAL

- 326 **Duplicated and Ectopic Ureter**
Amir A. Borhani, MD
- 330 **Ureterocele**
Amir A. Borhani, MD

INFLAMMATION

- 334 **Ureteritis Cystica**
Amir A. Borhani, MD and Michael P. Federle, MD, FACR
- 336 **Ureteral Stricture**
Amir A. Borhani, MD
- 338 **Malakoplakia**
Amir A. Borhani, MD

TRAUMA

- 340 **Ureteral Trauma**
Matthew T. Heller, MD, FSAR and Michael P. Federle, MD, FACR

NEOPLASMS

- 344 **Polyps**
Amir A. Borhani, MD
- 346 **Ureteral Transitional Cell Carcinoma**
Amir A. Borhani, MD

MISCELLANEOUS

- 350 **Ureterectasis of Pregnancy**
Amir A. Borhani, MD

SECTION 6: BLADDER

- 354 **Introduction to the Bladder**
Amir A. Borhani, MD and Paula J. Woodward, MD

CONGENITAL

- 358 **Urachal Anomalies**
Amir A. Borhani, MD and Michael P. Federle, MD, FACR

INFECTION

- 362 **Cystitis**
Amir A. Borhani, MD
- 364 **Bladder Schistosomiasis**
Amir A. Borhani, MD

DEGENERATIVE

- 366 **Bladder Calculi**
Amir A. Borhani, MD and Michael P. Federle, MD, FACR
- 368 **Bladder Diverticulum**
Amir A. Borhani, MD
- 372 **Fistulas of the Genitourinary Tract**
Amir A. Borhani, MD and Michael P. Federle, MD, FACR
- 376 **Neurogenic Bladder**
Amir A. Borhani, MD and Michael P. Federle, MD, FACR

TRAUMA

- 380 **Bladder Trauma**
Matthew T. Heller, MD, FSAR and Michael P. Federle, MD, FACR

TREATMENT RELATED

- 384 **Postoperative State, Bladder**
Amir A. Borhani, MD

BENIGN NEOPLASMS

- 388 **Mesenchymal Bladder Neoplasms**
Amir A. Borhani, MD
- 392 **Bladder Inflammatory Pseudotumor**
Amir A. Borhani, MD
- 394 **Bladder and Ureteral Intramural Masses**
Amir A. Borhani, MD

MALIGNANT NEOPLASMS

- 398 **Urinary Bladder Carcinoma**
Akram M. Shaaban, MBBCh
- 416 **Squamous Cell Carcinoma**
Amir A. Borhani, MD
- 418 **Adenocarcinoma**
Amir A. Borhani, MD

SECTION 7: URETHRA/PENIS

- 422 **Introduction to the Urethra**
Matthew T. Heller, MD, FSAR and Paula J. Woodward, MD

NEOPLASMS

- 424 **Urethral Carcinoma**
Christine O. Menias, MD

TABLE OF CONTENTS

INFECTION

- 436 **Urethral Stricture**
Matthew T. Heller, MD, FSAR and Michael P. Federle, MD, FACR
- 438 **Urethral Diverticulum**
Matthew T. Heller, MD, FSAR

TRAUMA

- 442 **Urethral Trauma**
Matthew T. Heller, MD, FSAR and Amir A. Borhani, MD
- 444 **Erectile Dysfunction**
Matthew T. Heller, MD, FSAR

SECTION 8: TESTES

NONNEOPLASTIC CONDITIONS

- 448 **Approach to Scrotal Sonography**
Shweta Bhatt, MD
- 450 **Cryptorchidism**
Paula J. Woodward, MD
- 452 **Testicular Torsion**
Shweta Bhatt, MD and Mitchell Tublin, MD
- 456 **Segmental Infarction**
Mitchell Tublin, MD
- 458 **Tubular Ectasia**
Mitchell Tublin, MD and Shweta Bhatt, MD
- 460 **Testicular Microlithiasis**
Mitchell Tublin, MD and Shweta Bhatt, MD

NEOPLASMS

- 464 **Germ Cell Tumors**
Mitchell Tublin, MD and Shweta Bhatt, MD
- 468 **Testicular Carcinoma Staging**
David Bauer, MD and Akram M. Shaaban, MBBCh
- 480 **Stromal Tumors**
Shweta Bhatt, MD and Mitchell Tublin, MD
- 484 **Testicular Lymphoma and Leukemia**
Shweta Bhatt, MD
- 486 **Epidermoid Cyst**
Mitchell Tublin, MD and Shweta Bhatt, MD

SECTION 9: EPIDIDYMIS

- 490 **Epididymitis**
Mitchell Tublin, MD and Shweta Bhatt, MD and Amit B. Desai, MD
- 494 **Adenomatoid Tumor**
Katherine E. Maturen, MD, MS
- 496 **Spermatocele/Epididymal Cyst**
Katherine E. Maturen, MD, MS
- 498 **Sperm Granuloma**
Mitchell Tublin, MD

SECTION 10: SCROTUM

- 502 **Hydrocele**
Mitchell Tublin, MD and R. Brooke Jeffrey, MD
- 504 **Varicocele**
Mitchell Tublin, MD and R. Brooke Jeffrey, MD

- 506 **Pyocele**
R. Brooke Jeffrey, MD
- 508 **Hernia**
Amir A. Borhani, MD
- 512 **Fournier Gangrene**
Mitchell Tublin, MD
- 514 **Scrotal Trauma**
Mitchell Tublin, MD and Shweta Bhatt, MD

SECTION 11: SEMINAL VESICLES

- 520 **Congenital Lesions**
Amir A. Borhani, MD
- 522 **Acquired Seminal Vesicle Lesions**
Amir A. Borhani, MD

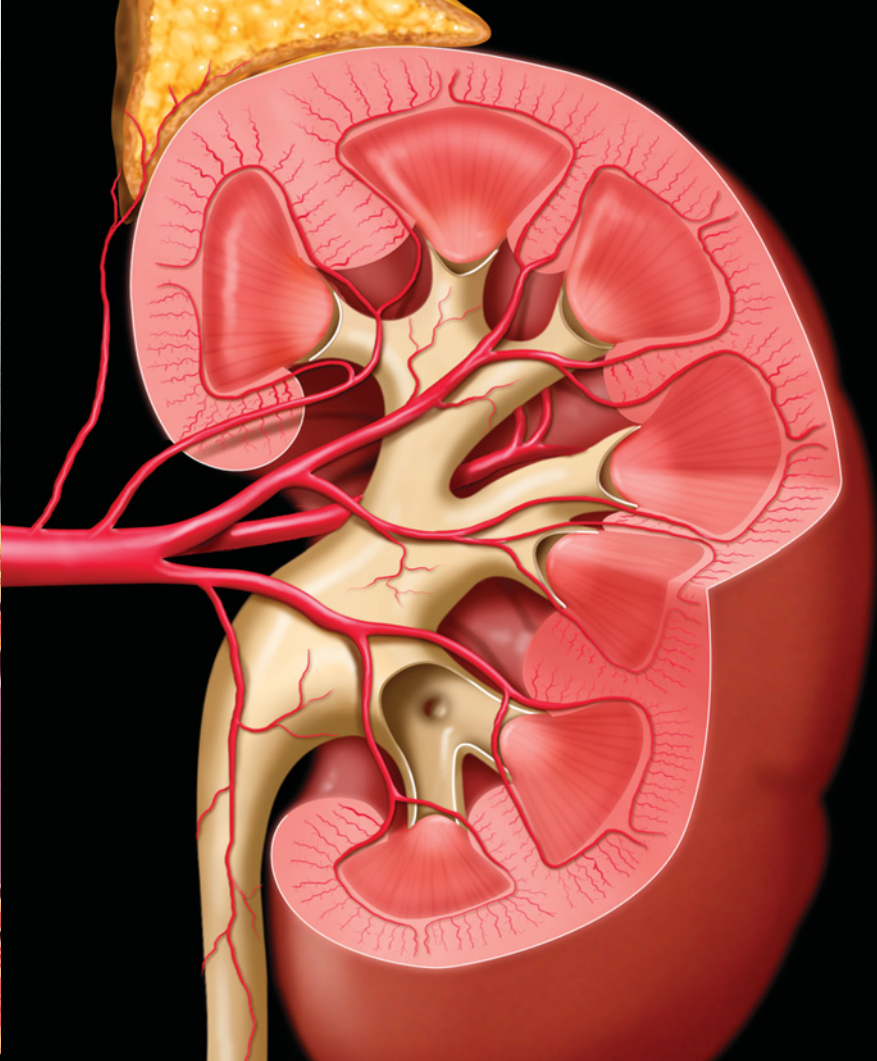
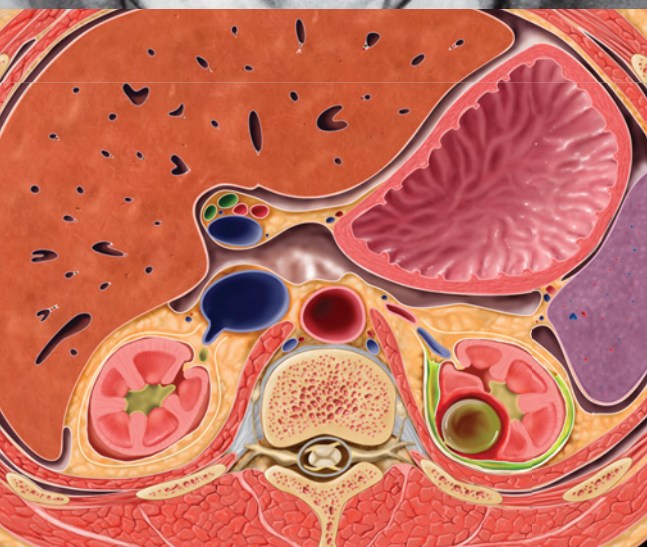
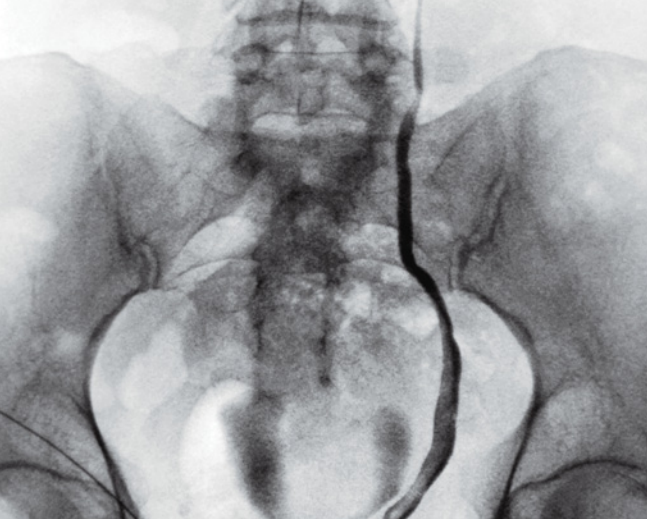
SECTION 12: PROSTATE

- 528 **Prostatitis and Abscess**
Alessandro Furlan, MD and Paula J. Woodward, MD
- 530 **Benign Prostatic Hypertrophy**
Alessandro Furlan, MD and R. Brooke Jeffrey, MD
- 532 **Prostatic Cyst**
Alessandro Furlan, MD and Paula J. Woodward, MD
- 534 **Prostate Carcinoma**
Alessandro Furlan, MD
- 540 **Prostate Carcinoma Staging**
Marta Heilbrun, MD, MS

SECTION 13: PROCEDURES

- 554 **Percutaneous Genitourinary Interventions**
Matthew T. Heller, MD, FSAR and Ashraf Thabet, MD
- 566 **Kidney Ablation/Embolization**
Mitchell Tublin, MD and Ashraf Thabet, MD
- 578 **Post Kidney Transplant Procedures**
Mitchell Tublin, MD and Ashraf Thabet, MD
- 590 **Venous Sampling and Venography (Renal and Adrenal)**
Amir A. Borhani, MD and T. Gregory Walker, MD, FSIR
- 594 **Fertility and Sterility Interventions**
Gloria M. Salazar, MD

This page intentionally left blank

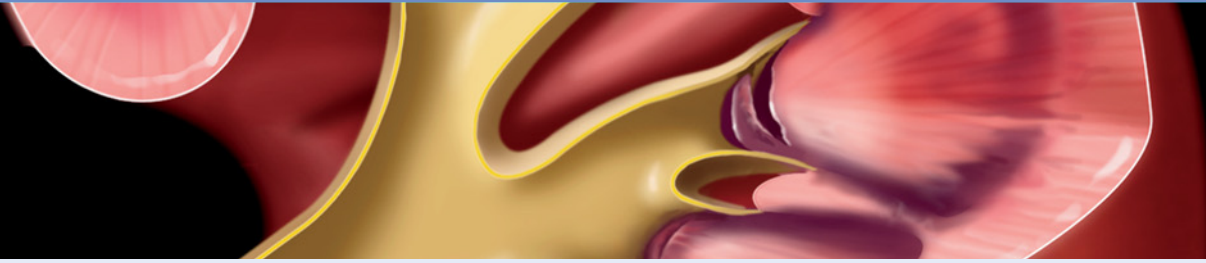


Diagnostic Imaging
Genitourinary

THIRD EDITION

This page intentionally left blank

SECTION 1
Overview and Introduction



Imaging Approaches

4

Renal Mass Evaluation

CT: Although rapid improvements in scanner technology have resulted in dramatic increases in spatial and temporal resolution, the imaging marker for potential neoplasia (enhancement of soft tissue components of renal masses after contrast administration) has not changed over several generations of CT scanners. Typical renal mass protocols consist of NECT of the kidneys followed by contrast-enhanced images obtained during nephrographic and excretory phases (roughly defined as 85-120 seconds and 3-5 minutes, respectively, post-contrast injection). Corticomedullary phase images (25-70 seconds post contrast) may also be obtained, though small, central, endophytic tumors may not be perceived given the lack of medullary enhancement during this phase. An increase in soft tissue attenuation of soft tissue components post-contrast administration of > 10-20 Hounsfield units (HU) is classically considered to be indicative of true enhancement, though "pseudoenhancement" of small lesions may result in false-positive examinations, and slowly enhancing lesions (e.g., papillary carcinomas) may be missed if delayed images are not acquired. Despite these caveats, if such a protocol is employed, most renal masses can be accurately characterized as potential surgical lesions (i.e., enhancing: Benign/malignant neoplasia), or leave-alone entities (either fat-containing angiomyelolipomas or simple-/high-attenuation cysts). Assessment of cyst complexity at CT, utilizing features described by Bosniak a generation ago, also aids in the triage of this particularly problematic category of renal masses. Suffice to say that increasing levels of complexity (septa thickness, wall/nodularity enhancement, and calcification) increase the likelihood of malignancy.

Optimized protocols should utilize the advantages of multidetector technology. Thin (.625-1.25 mm) source images are acquired and thicker (e.g., 2.5 mm) axial, coronal images are reconstructed. Such protocols allow for diagnostic coronal reconstructed image sets with isotropic or near isotropic resolution; these are particularly helpful for staging of renal cell carcinoma. The potential utility of dual energy for the characterization of renal masses is a topic of current intense investigation. These platforms may permit assessment of enhancement by calculating iodine concentration in the mass, though criteria for meaningful changes have not been universally accepted. The reproducibility of post-processed HU calculations will also need to be validated.

MR: Lesion enhancement is the feature that is also primarily assessed with tailored renal MR protocols. MR offers several unique advantages: Numerous fat-saturation T1-weighted dynamic enhanced phases can be obtained directly in a coronal plane, and dedicated Gadolinium (Gd)-enhanced delayed coronal imaging is the standard of care for identification and characterization of renal vein-caval thrombus. Chemical shift imaging and frequency selective fat-saturation technique may be utilized to identify the fat that is characteristic of angiomyelolipomas. Assessment of T2 and T1 signal intensity improves diagnostic accuracy: Enhancing T2-hyperintense lesions are likely renal cell carcinomas, whereas enhancing T2-hypointense lesions are typically either nonfat-containing AMLs or papillary renal cell carcinoma. Diffusion-weighted imaging assessment may also be employed, though the apparent diffusion coefficient (ADC) value overlap between benign and malignant renal lesions has limited the utility of this technique. A final caveat regarding MR assessment of renal masses is that gadolinium enhancement

of renal masses on MR remains a largely qualitative biomarker of neoplasia (though one that is better assessed by evaluating subtracted images).

Ultrasound: Despite marked improvements in ultrasound platforms over the past 40 years, the role of ultrasound in the renal mass imaging algorithm has not changed: Ultrasound is typically performed to determine if a lesion is cystic or solid. Technique should be optimized: Compound and harmonic imaging should be routinely employed to reduce artifacts and to obtain sufficient penetration. Color Doppler may be utilized to help identify pseudolesions (e.g., column of Bertin, renal scars) and rarely, to identify flow within solid or complex cystic masses. Microbubble contrast agents have been employed in several centers to increase the accuracy of ultrasound assessment of renal masses: Unlike CT and MR, enhancement of masses may be observed at continuous real-time examination using low mechanical index protocols, although standards for enhancement are not uniform, and FDA approval for this indication is still forthcoming.

Hematuria (and Potential Urothelial Malignancy) Evaluation

CT urography (CTU): CTU has supplanted conventional intravenous urography as the noninvasive imaging gold standard for the evaluation of patients with hematuria when nephrologic causes (e.g., urinary tract infection, glomerulonephritis) have been excluded. Nonetheless, societies differ on age cutoffs for its use and whether ultrasound may be employed as a primary screen in selected, typically younger, populations. Guidelines for optimizing CTU also widely differ. The basic CTU study includes an initial NECT (to assess for calculi and as a baseline for assessing lesion enhancement if ultimately present), a nephrographic phase for identification of potential renal lesions, and an excretory phase for depicting upper and lower tracts. Coverage and imaging technique may vary, though 64-slice MDCT should be employed to obtain thin-slice source images for multiplanar and MIP reconstructions. Approaches to minimize radiation dosing include multiple new iterative reconstruction algorithms, selective coverage, and split-bolus protocols. CTU performed with dual energy scanners may be a theoretically attractive option to decrease dosing because a virtual NECT may be obtained, though punctate calculi are sometimes obscured. Finally, several options to optimize ureteral opacification (oral hydration, saline administration, low-dose diuretics, prone positioning, and compression) have been employed, but comparison of efficacy between studies is difficult, results have varied, and the logistics of several of these techniques can be daunting. Many centers continue to use simple oral hydration with 1 liter of water 30-60 minutes prior to imaging, and a 3-phase protocol with satisfactory results.

MR urography (MRU): MRU is employed in some centers for evaluation of upper tract malignancy and for identification of urinary tract anomalies. A typical MR urogram includes static fluid heavily T2-weighted sequences and excretory T1-weighted images after gadolinium administration. Like with CTU, saline &/or diuretic administration may improve contrast distribution throughout upper tracts. The renal parenchyma is screened with T1-, T2-weighted images and nephrographic phase Gd-enhanced MR. An abbreviated static T2 MRU protocol may be performed in patients with renal insufficiency to avoid the potential risk of nephrogenic system sclerosis.

Such an approach may also be a viable alternative for pregnant patients with potential renal colic. Use of dedicated phase array coils improves resolution, though it should be noted that both static T2-weighted MR and excretory T1-weighted MR are prone to motion artifact and lack the spatial resolution of CTU; identification of small calculi may be particularly problematic.

Intravenous urography, retrograde urography: Intravenous urography is rarely performed; it includes tomographic images obtained approximately 1 minute post-contrast administration and delayed views of the kidneys, ureters, and bladder. Problematic areas may be evaluated at fluoroscopy and compression improves upper tract distention. Retrograde urography is invasive, though it provides a necessary road map for cystoscopic procedures and may be helpful for confirmation of equivocal lesions suggested at either CTU or MRU.

Renal Dysfunction Evaluation

Ultrasound: Ultrasound is the modality typically employed during the initial assessment of the patient with renal insufficiency. Collecting system dilatation, renal size, symmetry, and echogenicity are easily assessed. The utility of ultrasound in nonselected patients in the acute setting has been called into question, however; the likelihood of bilateral ureteral obstruction (manifested by hydronephrosis at ultrasound) in patients without a prior history of hydronephrosis, abdominal/pelvic malignancy, or pelvic surgery is extremely low. An additional limitation of the modality is that it is an anatomic test; it is impossible to differentiate between obstructive and nonobstructive pelvicaliectasis based upon ultrasound alone.

Preliminary work in the radiology literature, subsequently built upon by other disciplines, has suggested a role for Doppler in assessing the changes in renal hemodynamics that occur with varying causes of renal dysfunction. Most papers have employed the resistive index (RI) (peak systolic velocity/end diastolic velocity/peak systolic velocity) as a surrogate for renal vascular resistance. Recent work has shown, however, how changes in segmental renal arterial RIs are due to tissue compliance (not vascular resistance) and that the RI is neither a specific nor sensitive parameter for the many causes of renal failure. Advocates for contrast-enhanced ultrasound have recently proposed a more elegant ultrasound approach for assessing renal physiology: Tissue perfusion (not flow velocities assessed by Doppler) may be calculated by analyzing replenishment kinetics after bubbles are transiently destroyed by a high mechanical index pulse. However, these techniques have not been adopted by practices outside of select research centers given the lack of FDA approval of microbubble agents and the logistics involved with bubble studies. Despite these limitations, the low cost, portability, and lack of radiation associated with ultrasound have solidified its central longstanding role in the evaluation of the patient with renal dysfunction. Ultrasound is also used for renal biopsy guidance in those patients in whom renal dysfunction is unexplained and persistent.

CT: Like with ultrasound, traditional CT largely evaluates gross anatomic causes for renal failure. It may be helpful for depicting obstructing pelvic malignancies or infiltrating renal neoplastic or inflammatory processes. Several centers have assessed the potential role of MDCT for extracting functional parameters (renal perfusion, renal blood flow, and glomerular

filtration) from renal time-density curves obtained during intravenous contrast administration. Patlak modeling of renal contrast kinetics has shown promise in evaluating the pathophysiology of a variety of renal diseases, but the need for central venous line placement, radiation exposure, and (most importantly) large IV contrast doses for renal contrast kinetic studies has prevented its use in patients with preexisting renal dysfunction.

MR: Gd contrast kinetics may also be analyzed to assess split renal function and global glomerular filtration rate (GFR), although like with CT function studies, these approaches have not been validated in large-scale studies. The length of the examination, reproducibility issues, motion artifact, and the potential of Gd agents to induce nephrogenic systemic fibrosis in patients with renal disease have limited the utility of Gd-enhanced renal function studies. Nonenhanced functional MR approaches may ultimately be incorporated into clinical practice; however, diffusion-weighted MR has been proposed as a noninvasive exam for identifying renal fibrosis, and blood oxygen level-dependent (BOLD) MR techniques may assess changes in renal and cortical oxygen tension (and, by extension, renal blood flow).

Nuclear medicine: Various nuclear medicine techniques are still employed to assess renal function. Tc-99m MAG3 is the agent of choice for dynamic radionuclide renal imaging at most centers. Clearance of this agent is primarily via tubular secretion. Renograms can be evaluated to assess urinary uptake, transit, excretion, and split renal function. Lasix renography may be employed to help differentiate between obstructive and nonobstructive pelvicaliectasis. Changes in renogram curves after administration of captopril (an angiotensin-converting enzyme inhibitor) may be helpful for detecting renovascular hypertension and assessing the impact of surgical or angiographic intervention. Tc-99m DMSA is still the preferred radiopharmaceutical for static parenchymal imaging. This agent concentrates within the renal cortex and best shows functioning tubular mass. As such, it is useful for assessing renal scarring (due to urinary tract infections or reflux nephropathy) and calculating relative renal function. Finally, a variety of radionuclide techniques for GFR estimation may be employed, although in routine clinical practice, estimates of GFR are typically made using equations that incorporate serum creatinine, weight, and multiple additional readily measured parameters. It should be noted that, despite their widespread use, all of these equations (including the most commonly employed Modification of Diet in Renal Disease [MDRD] formula) are limited in patients with unstable renal function. Estimates in certain populations (e.g., cirrhotic or pregnant patients) may be particularly prone to error.

Adrenal Mass Evaluation

CT: The high incidence of incidental adrenal masses has prompted a variety of imaging approaches for their characterization. The work-up of these often asymptomatic lesions (or adrenal “incidentalomas”) remains imaging intensive, despite large-scale retrospective studies that have shown that the vast majority of small (< 4 cm), incidental adrenal lesions identified at cross-sectional imaging are benign (i.e., adrenal adenomas, cysts, myelolipomas).

Two basic approaches for characterizing adrenal masses at CT are utilized. The attenuation of the adrenal lesion at NECT is assessed. An attenuation of < 10 HU is highly specific for an adenoma (due to the high lipid content of most adenomas).

Attenuation of < 10 HU might also suggest a true endothelial or post-traumatic pseudocyst (another typically benign lesion). Although differentiation between simple cysts and adenomas is usually not clinically relevant, thin wall calcification is a common feature of cysts.

The small percentage of adenomas that do not contain much intracellular lipid may be identified by evaluating contrast kinetics. The washout of contrast from so-called lipid-poor adenomas is typically brisk, as opposed to metastases. Delayed absolute or relative washout of iodinated contrast may be calculated using readily available web-based calculators. Brisk washout may also be seen in a small percentage of pheochromocytomas and vascular metastases (e.g., renal cell carcinoma, hepatocellular carcinoma), although in these cases, an appropriate endocrine evaluation and clinical history may help avoid an errant diagnosis of an adenoma. Finally, the incidental large (> 4 cm) but imaging benign adrenal mass remains a management dilemma. Current dogma continues to suggest that in appropriate surgical candidates, these lesions should be resected given the concern for adrenal cortical carcinoma.

MR: Like NECT, chemical shift MR is employed to identify the lipid content of adrenal adenomas. Relative percent signal suppression at out-phase imaging may be used to increase diagnostic confidence, but qualitative assessment often suffices. Early MR studies suggested a role of MR for identifying pheochromocytomas, but the classic “light bulb” T2-bright appearance is neither a sensitive nor specific feature of these lesions.

Bladder Mass Evaluation

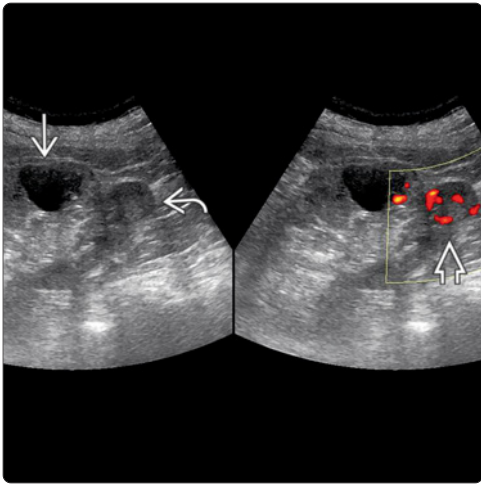
CT: The sensitivity and specificity of CTU for the diagnosis of bladder cancer in patients with hematuria is over 90%. MDCT is readily available, and the recommendations of multiple societies have highlighted its effectiveness in assessing visceral and nodal metastases pre and post therapy. Even well-performed, state of the art MDCT often fails with local T staging, however. The depth of muscle invasion is frequently under- or overestimated, though CT performs better with higher T score tumors. Thus, cystoscopy remains in every algorithm of the investigation of hematuria. Imaging-suspected or occult bladder lesions are directly visualized, and if present, biopsy for diagnosis and depth of invasion is performed. Similarly, size and shape remain the only imaging criteria for nodal metastases, and like with other GU malignancies, low-volume nodal disease will not be identified. Recent work has also unfortunately suggested that PET/CT adds little beyond conventional MDCT to local N staging.

MR: The role of MR for the local staging of bladder cancer continues to evolve. The superior soft tissue contrast resolution of MR using standard T1-, T2-weighted imaging sequences allows for better differentiation between bladder wall layers. Multiple studies have shown that compared to CT, MR performs better for identifying intramural tumor invasion and perivesical spread. Nonetheless, MR often fails, and muscle invasion may be under or over called. Multiparametric imaging (combining multiplanar T1/T2 image sets, diffusion-weighted MR, and dynamic contrast-enhanced MR) may improve staging accuracy, though this approach is currently employed at select centers. Preliminary work has also

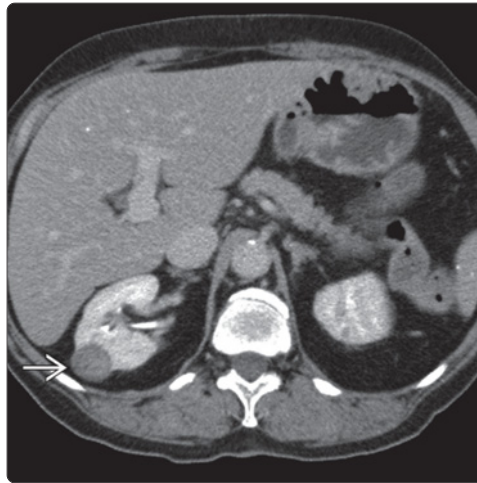
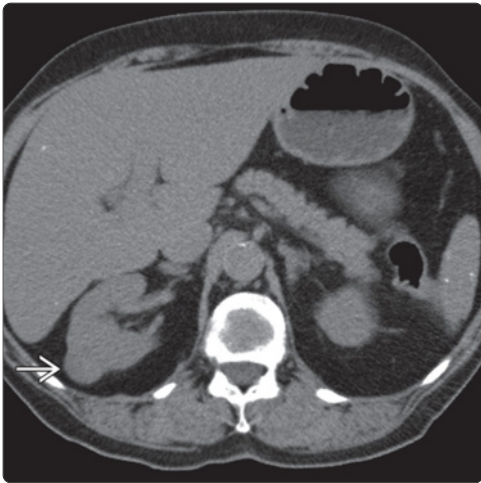
suggested the utility of ultra small super paramagnetic iron oxide (USPIO) particles and diffusion MR for node characterization, though for the meantime, radical cystectomy and extended template node dissection remain the standard of care for the staging and therapy of confirmed muscle invasive tumor.

Selected References

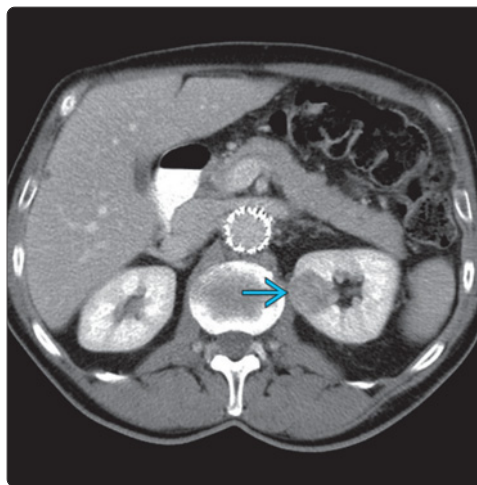
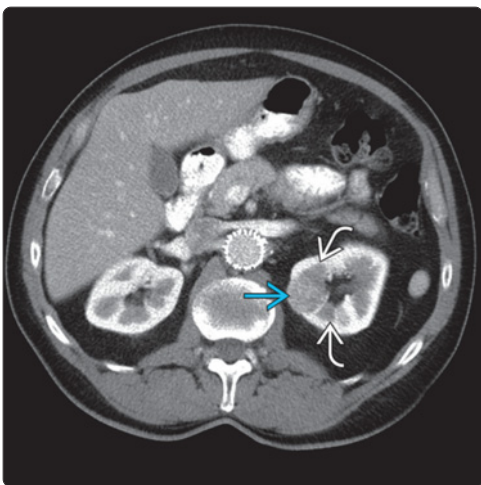
- Ioachimescu AG et al: Adrenal Incidentalomas: A disease of modern technology offering opportunities for improved patient care. *Endocrinol Metab Clin North Am.* 44(2):335-354, 2015
- Davarpanah AH et al: MR imaging of the kidneys and adrenal glands. *Radiol Clin North Am.* 52(4):779-98, 2014
- Heller MT et al: In search of a consensus: evaluation of the patient with hematuria in an era of cost containment. *AJR Am J Roentgenol.* 202(6):1179-86, 2014
- McClellan BL: Imaging the renal mass: a historical review. *Radiology.* 273(2 Suppl):S126-41, 2014
- Kaza RK et al: Dual-energy CT of the urinary tract. *Abdom Imaging.* 38(1):167-79, 2013
- Lawrentschuk N et al: Current role of PET, CT, MR for invasive bladder cancer. *Curr Urol Rep.* 14(2):84-9, 2013
- Raman SP et al: MDCT evaluation of ureteral tumors: advantages of 3D reconstruction and volume visualization. *AJR Am J Roentgenol.* 201(6):1239-47, 2013
- Wolin EA et al: Nephrographic and pyelographic analysis of CT urography: differential diagnosis. *AJR Am J Roentgenol.* 200(6):1197-203, 2013
- Wolin EA et al: Nephrographic and pyelographic analysis of CT urography: principles, patterns, and pathophysiology. *AJR Am J Roentgenol.* 200(6):1210-4, 2013
- Verma S et al: Urinary bladder cancer: role of MR imaging. *Radiographics.* 32(2):371-87, 2012
- Siegelman ES: Adrenal MRI: techniques and clinical applications. *J Magn Reson Imaging.* 36(2):272-85, 2012
- Taffel M et al: Adrenal imaging: a comprehensive review. *Radiol Clin North Am.* 50(2):219-43, v, 2012
- Chandarana H et al: Iodine quantification with dual-energy CT: phantom study and preliminary experience with renal masses. *AJR Am J Roentgenol.* 196(6):W693-700, 2011
- Durand E et al: Functional renal imaging: new trends in radiology and nuclear medicine. *Semin Nucl Med.* 41(1):61-72, 2011
- Grenier N et al: Radiology imaging of renal structure and function by computed tomography, magnetic resonance imaging, and ultrasound. *Semin Nucl Med.* 41(1):45-60, 2011
- Kaza RK et al: Distinguishing enhancing from nonenhancing renal lesions with fast kilovoltage-switching dual-energy CT. *AJR Am J Roentgenol.* 197(6):1375-81, 2011
- Notohamiprodjo M et al: Diffusion and perfusion of the kidney. *Eur J Radiol.* 76(3):337-47, 2010
- Israel GM et al: Pitfalls in renal mass evaluation and how to avoid them. *Radiographics* 28: 1325-1338; 2008
- Quaia E et al: Comparison of contrast-enhanced sonography with unenhanced sonography and contrast-enhanced CT in the diagnosis of malignancy in complex cystic renal masses. *AJR Am J Roentgenol.* 191(4):1239-49, 2008
- Setty BN et al: State-of-the-art cross-sectional imaging in bladder cancer. *Curr Probl Diagn Radiol.* 36(2):83-96, 2007
- O'Connor OJ et al: MR Urography. *AJR Am J Roentgenol.* 195(3):W201-6, 2010
- Silverman SG et al: Hyperattenuating renal masses: etiologies, pathogenesis, and imaging evaluation. *Radiographics.* 27(4):1131-43, 2007
- Tublin ME et al: Review. The resistive index in renal Doppler sonography: where do we stand? *AJR Am J Roentgenol.* 180(4):885-92, 2003





(Left) Grayscale and power Doppler renal ultrasound performed on a patient with renal insufficiency shows a cyst [black arrow] and an incidental isoechoic lower pole renal cell carcinoma (RCC) [white arrow]. Ultrasound is typically performed to differentiate solid from cystic lesions. Intralesional Doppler flow [red arrows] helps confirm malignancy. (Right) Ultrasound shows an echogenic RCC [white arrow]. Differentiating between an echogenic RCC and AML may be difficult on ultrasound, but a thin halo [black arrow] and the lack of weak shadowing favor RCC.

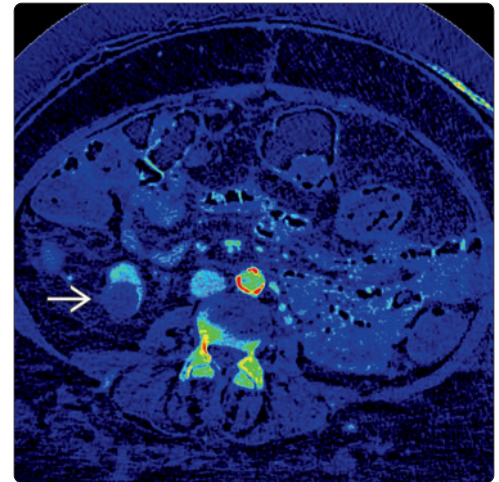
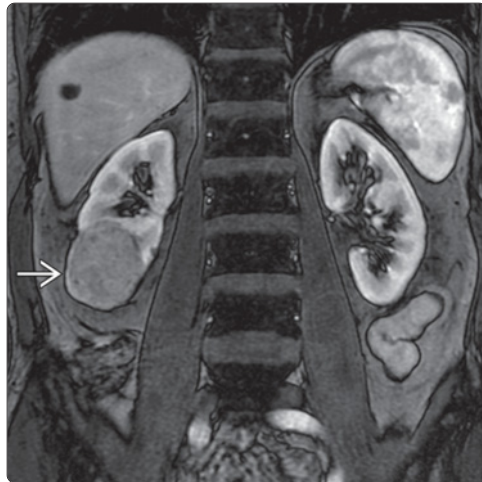




(Left) NECT shows an exophytic solid attenuation right renal lesion [white arrow]. Either ultrasound or CECT is needed to differentiate between a high-attenuation cyst and solid neoplasia. (Right) CECT of the same patient performed during the nephrographic phase shows that the lesion [white arrow] enhances by 40 HU. Enhancement is the hallmark imaging marker of neoplasia. Papillary renal cell carcinoma was confirmed at laparoscopic partial nephrectomy.




(Left) CECT performed during the corticomedullary shows a subtle, largely non-border-deforming left upper pole renal lesion [white arrow]. Its attenuation is similar to minimally enhanced surrounding medulla [blue arrow]. (Right) CECT of the same patient during the nephrographic phase shows an obvious, now relatively low-attenuation left upper pole mass [white arrow] (confirmed clear cell RCC). Endophytic renal masses are often imperceptible on the corticomedullary phase. De-enhancement of masses over time is an additional imaging marker of neoplasia.

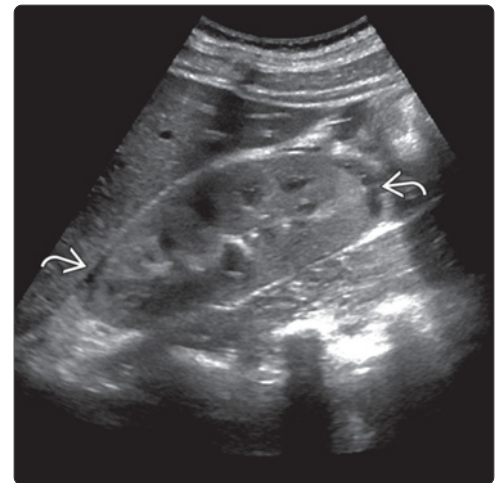
(Left) Gd-enhanced T1WI MR shows an exophytic right lower pole RCC . Assessment of contrast enhancement at MR is largely qualitative; subtraction images may be helpful in problematic cases. **(Right)** DECT spectral data is used to generate an iodine-specific overlay map. Qualitative assessment confirms no iodine uptake in a high-attenuation right renal cyst . Early work has suggested that direct quantification of iodine concentration may compete with HU assessment of neoplasia enhancement.



(Left) Gd-enhanced T1WI MR shows expansile, enhancing tumor thrombus  within the left renal vein in a patient with an adjacent RCC (not shown). Coronal imaging is particularly helpful for the preoperative evaluation of T3 RCC. **(Right)** CT urogram in an elderly man with hematuria shows an infiltrating right renal urothelial cell carcinoma . Recent consensus statements advocate CTU for the evaluation of non-nephrologic causes of hematuria, though age guidelines and the utility of ultrasound are still debated.

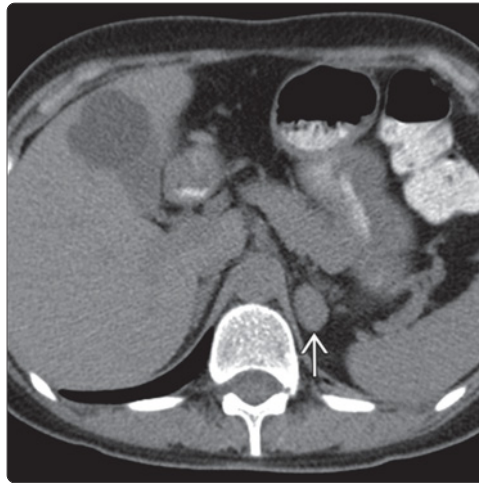
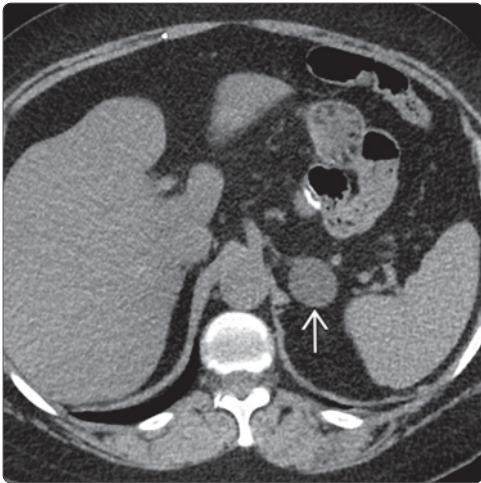


(Left) Gd-enhanced T1W urogram shows normal upper tracts. Both Gd-enhanced and heavily T2-weighted sequences are part of typical MRU protocols, though image resolution is less than that obtained by CT urography and calculi may not be identified. **(Right)** Ultrasound of a patient with acute renal failure shows a normal-sized echogenic kidney (a nonspecific finding of medical renal disease) and perirenal edema . The primary role of ultrasound in this setting is to assess renal size and collecting system dilatation.

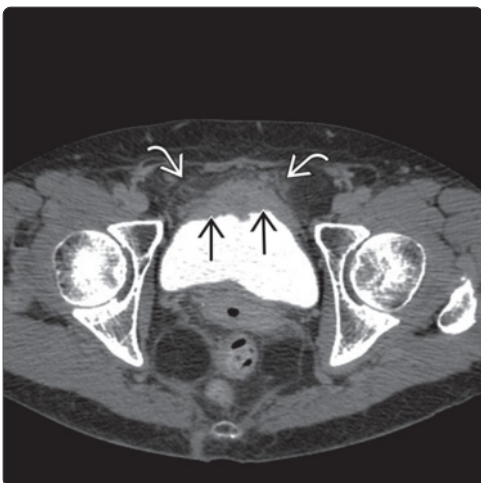




(Left) In phase T1WI MR in a 37-year-old woman with Cushing syndrome shows an intermediate signal intensity left adrenal lesion \Rightarrow . (Right) Out of phase T1WI MR of the same patient shows uniform signal loss of a lipid-rich adenoma \Rightarrow . Chemical shift imaging exploits resonance differences between lipid and water to detect the intracytoplasmic fat characteristic of lipid-rich adenomas. Adrenal to spleen suppression ratios may be calculated for problematic cases, but visual assessment typically suffices.



(Left) NECT of a patient with Cushing syndrome shows a left adrenal lesion \Rightarrow measuring -2 HU. NECT is an effective screening modality for characterizing lipid-rich adenomas, but the utility of intensive imaging for incidental adrenal lesions has been questioned. (Right) Baseline NECT shows an incidental, indeterminate, left adrenal mass \Rightarrow . Relative and absolute washout percentages on a dedicated adrenal CT (not shown) confirmed a lipid-poor adenoma. Web-based programs are readily available for calculations.

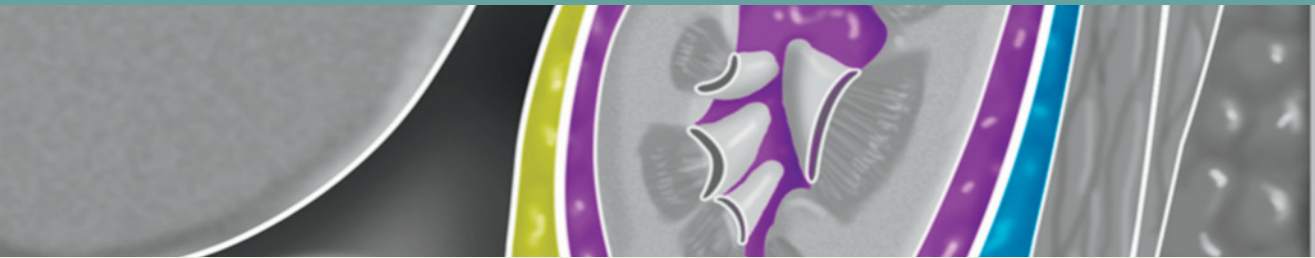


(Left) Delayed CECT shows a large, sessile, anterior bladder urothelial carcinoma \Rightarrow . Prevesical fat infiltration \Rightarrow suggests T3 tumor (i.e., tumor extending beyond detrusor). CT is utilized for preoperative evaluation of nodal and visceral metastases, but it is typically not helpful for assessing tumor depth (T stage). (Right) Sagittal T2WI MR shows a likely muscle-confined (T2) bladder dome urachal adenocarcinoma \Rightarrow . MR performs better than CT for assessing tumor depth, but cystoscopic biopsy remains the standard of care for T staging.

This page intentionally left blank

SECTION 2

Retroperitoneum



Introduction to the Retroperitoneum	12
Congenital	
Duplications and Anomalies of IVC	16
Inflammation	
Retroperitoneal Fibrosis	20
Degenerative	
Pelvic Lipomatosis	24
Treatment Related	
Coagulopathic (Retroperitoneal) Hemorrhage	26
Postoperative Lymphocele	30
Benign Neoplasms	
Retroperitoneal Neurogenic Tumor	32
Malignant Neoplasms	
Retroperitoneal Sarcoma	36
Retroperitoneal and Mesenteric Lymphoma	40
Retroperitoneal Metastases	44
Hemangiopericytoma	48
Perivascular Epithelioid Cell Tumor (PEComa)	50

Relevant Anatomy and Embryology

The parietal peritoneum separates the peritoneal cavity from the retroperitoneum. The retroperitoneum contains all the abdominal contents located between the parietal peritoneum and the transversalis fascia. It is divided into 3 compartments by 2 well-defined fascial planes: The renal and lateroconal fasciae.

The **perirenal space** contains the kidney, adrenal, proximal ureter, and abundant fat and it is enclosed by the renal fascia, which is also referred to as Gerota fascia. The 2 perirenal spaces do not communicate across the abdominal midline.

The **anterior pararenal space** contains the pancreas, duodenum, colon (ascending and descending), and a variable amount of fat.

The **posterior pararenal space** contains fat but no organs; it is contiguous with the properitoneal fat along the flanks.

The anterior renal fascia separates the perirenal space from the anterior pararenal space, and the posterior renal fascia separates the perirenal space from the posterior pararenal space.

The lateroconal fascia separates the anterior from the posterior pararenal space and marks the lateral extent of the anterior pararenal space.

The renal fascia joins and closes the perirenal space resembling an inverted cone with its tip in the iliac fossa. Caudal to the perirenal space, in the pelvis, the anterior and posterior pararenal spaces merge to form a single infrarenal retroperitoneal space, which communicates directly with the pelvic prevesical space (of Retzius). Due to an opening in the cone of the renal fascia caudally, the perirenal space communicates with the infrarenal retroperitoneal space. Thus, all 3 retroperitoneal compartments communicate with each other within the lower abdomen and pelvis. All of the pelvic retroperitoneal compartments, such as the perivesical and perirectal spaces, communicate with each other, which is evident and clinically relevant in cases of pelvic hemorrhage or tumor as well as with extraperitoneal rupture of the urinary bladder.

The renal and lateroconal fascia are laminated planes, which can split to form potential spaces as pathways of spread for rapidly expanding fluid collections or inflammatory processes, such as hemorrhage or acute pancreatitis. Splitting of the anterior renal fascia creates a "retromesenteric plane" that communicates across the midline; splitting of the posterior renal fascia creates a "retrorenal plane," which also communicates across the midline and anteriorly. Knowing this principle is crucial to understanding how disease originating in the anterior pararenal space, such as acute pancreatitis, can extend posterior to the back of the kidney or how fluid collections within the posterior pararenal space or retrorenal plane can extend around the lateral or even anterior abdominal wall.

Imaging Techniques and Indications

Multiplanar CT and MR are ideally suited to display the anatomy and pathology of retroperitoneal disease processes. Use of intravenous contrast material allows easier recognition of fascial plane landmarks and pathology and should be used unless contraindicated.

Approach to Retroperitoneal Abnormalities

Perirenal Space

Disease within the perirenal space is usually the result of diseases of the kidney. Common disease states include hemorrhage, infection, inflammation, and neoplasia.

The renal fascia is very strong and is usually effective in containing most primary renal pathology within the perirenal space. Similarly, it usually excludes most other processes from invading or involving the perirenal space.

The perirenal space is divided irregularly and inconsistently by perirenal bridging septa that often result in loculation of perirenal fluid, which may be misinterpreted as subcapsular in location. The perirenal septa also act as conduits for fluid or infiltrative disease, including tumor, to enter or leave the perirenal space.

Perirenal fluid may represent blood, urine, or pus or may be simulated by inflammation of the perirenal fat. Hemorrhage is often due to trauma, but may occur due to anticoagulation, rupture of a renal tumor, or vasculitis. Pus or inflammation usually originates from acute pyelonephritis, which may be associated with an abscess. Perirenal urine ("urinoma") may result from trauma with laceration through the renal collecting system, but it usually resolves rapidly unless there is an obstruction to the flow of urine to the bladder. Acute urine extravasation may also accompany ureteral obstruction by a calculus due to forniceal rupture.

Renal cell carcinoma is common, and the renal fascia usually confines the tumor, preventing invasion of contiguous structures. Spread to lymph nodes or hematogenous spread through the renal vein and inferior vena cava may occur and constitute important elements of the imaging and staging of this tumor.

Anterior Pararenal Space

Disease within the anterior pararenal space is common. For example, acute pancreatitis results in peripancreatic infiltration \pm fluid collections that spread throughout the anterior pararenal space, often affecting the duodenum and ascending and descending colon segments that share this anatomic compartment. The spread of inflammation is usually limited posteriorly by the anterior renal fascia, and laterally by the lateroconal fascia. Thickening of these planes is a reliable clue as to the presence of pancreatitis, which might otherwise be occult on imaging. The perirenal space is usually not involved in acute pancreatitis, sometimes resulting in a striking appearance of a perirenal "halo" of fat density while other retroperitoneal spaces and planes are infiltrated. Ventral (anterior) spread of inflammation or tumor from the anterior pararenal space is not limited by any fascial boundary, but only by the posterior parietal peritoneum. The root of the mesentery and transverse mesocolon originate from just ventral to the 3rd portion of duodenum and pancreas, and disease originating in these organs may easily dissect into the mesentery without crossing any anatomic boundaries. Some refer to the spaces enclosed by the mesenteric layers as the "subperitoneal space," emphasizing that there is no inviolate separation between the intraperitoneal and retroperitoneal spaces.

A duodenal ulcer may perforate and result in extraluminal gas and fluid that occupy 1 or more spaces, including the anterior pararenal, intraperitoneal (as the duodenal bulb is an intraperitoneal structure), and even the perirenal space since

the latter is open at the renal hilum and communicates with the anterior pararenal space.

Posterior Pararenal Space

Disease originating within the posterior pararenal space is uncommon, essentially limited to hemorrhage and tumor.

"Retroperitoneal hemorrhage" is a misnomer since most spontaneous, coagulopathic hemorrhage originates within the abdominal wall, the iliopsoas compartment, or the rectus sheath. Only when hemorrhage extends beyond these fascial boundaries does it enter the retroperitoneum. Rectus sheath hematomas enter the extraperitoneal pelvic spaces through a defect in the caudal (infraumbilical) portion of the sheath. Iliopsoas hemorrhage often extends into any or all of the retroperitoneal compartments, predominantly along the main fascial planes. The hallmarks of coagulopathic hemorrhage are: Bleeding out of proportion to trauma, multiple sites of bleeding, and the presence of the "hematocrit" sign, a fluid-cellular debris level within the hematoma.

Retroperitoneal sarcomas, most commonly liposarcoma, often originate within 1 of the retroperitoneal compartments, and the site of origin can be determined by the relative mass effect on various organs and structures such as the kidneys, colon, and great vessels. Most liposarcomas have some identifiable fat within them and seem to be encapsulated, allowing for excision, although recurrent disease is common.

If retroperitoneal nodes are included in the discussion, the most common retroperitoneal tumor is non-Hodgkin lymphoma (NHL). NHL often results in massive lymphadenopathy. This characteristically involves the mesenteric and retroperitoneal nodes that are confluent and anteriorly displace the aorta and inferior vena cava from the spine. Retroperitoneal nodes are also frequently involved by malignancies originating in pelvic organs, such as the prostate, rectum, and cervix.

The other large, though uncommon group of primary retroperitoneal tumors are of neurogenic origin, including nerve sheath tumors, ganglioneuroma, neuroblastoma, and others. These often share the characteristics of appearing as well-defined, moderately enhancing masses that do not appear to arise from nodes nor abdominal viscera. Many, in

fact, arise along the sympathetic nerve trunks, while others are part of a syndrome such as neurofibromatosis that may involve multiple nerves in a paraspinous or presacral distribution.

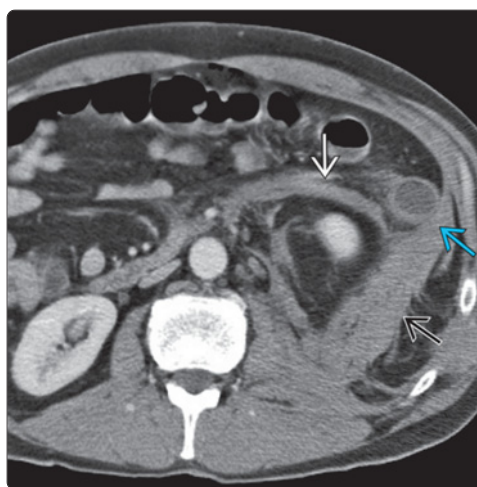
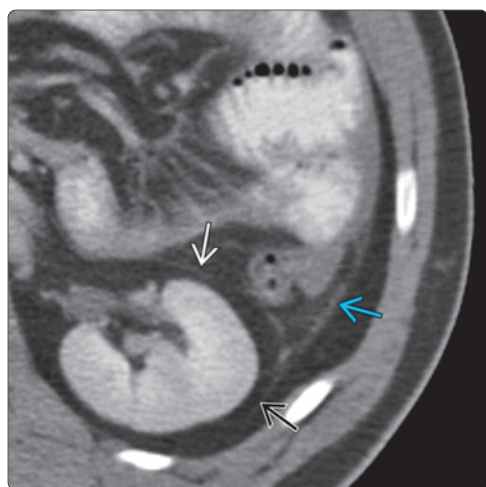
The great vessels, the aorta and inferior vena cava (IVC), are located in the retroperitoneum and are usually depicted as lying within the retromesenteric plane. Although primary disease of the IVC is rare, it may be the site of primary tumor (sarcoma) or the site of spread from a renal or adrenal carcinoma. More common are anomalies of the embryologic development of the IVC. Some 10% of the population have some anomaly of the embryologic sub- and supracardinal veins, usually at or below the level of the renal veins, resulting in variations such as duplicated IVC and retro- and circumaortic renal vein. While these are uncommonly of clinical significance (limited to affecting surgical and interventional procedures), they may be mistaken for pathologic conditions, most commonly enlarged retroperitoneal lymph nodes.







Abdominal aortic aneurysm is a major health concern, and rupture is usually fatal. Accurate diagnosis and precise mapping of the size and shape of an aneurysm allows effective, minimally invasive prophylactic treatment with endovascular stenting.

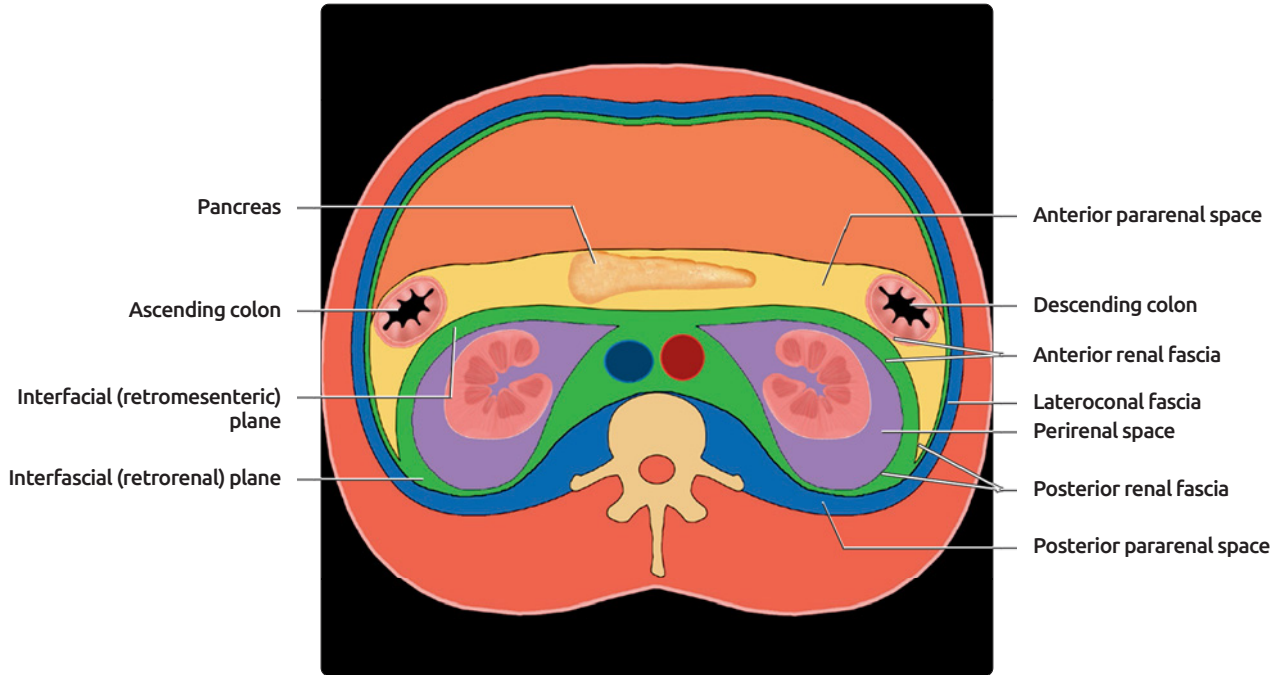
Retroperitoneal fibrosis is an inflammatory disorder that may be misinterpreted as a malignant process, as it envelops the aorta and IVC, often causing displacement and encasement of the ureters. It may occur as an isolated process or as part of a multisystem autoimmune disorder.

Selected References

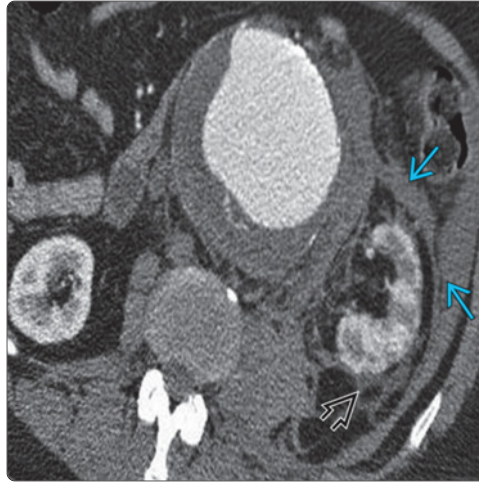
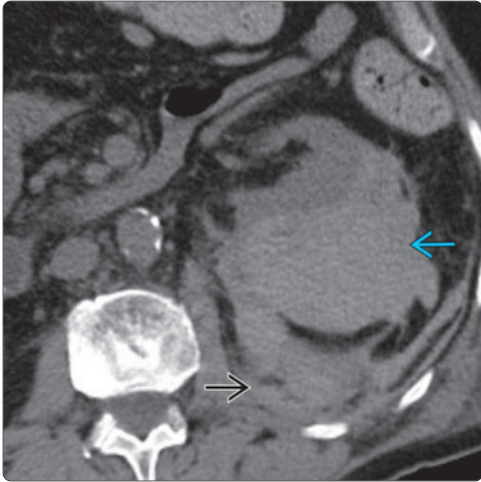
1. Osman S et al: A comprehensive review of the retroperitoneal anatomy, neoplasms, and pattern of disease spread. *Curr Probl Diagn Radiol.* 42(5):191-208, 2013
2. Goenka AH et al: Imaging of the retroperitoneum. *Radiol Clin North Am.* 50(2):333-55, vii, 2012
3. Tirkes T et al: Peritoneal and retroperitoneal anatomy and its relevance for cross-sectional imaging. *Radiographics.* 32(2):437-51, 2012
4. Lee SL et al: Comprehensive reviews of the interfascial plane of the retroperitoneum: normal anatomy and pathologic entities. *Emerg Radiol.* 17(1):3-11, 2010
5. Sanyal R et al: Radiology of the retroperitoneum: case-based review. *AJR Am J Roentgenol.* 192(6 Suppl):S112-7 (Quiz S118-21), 2009



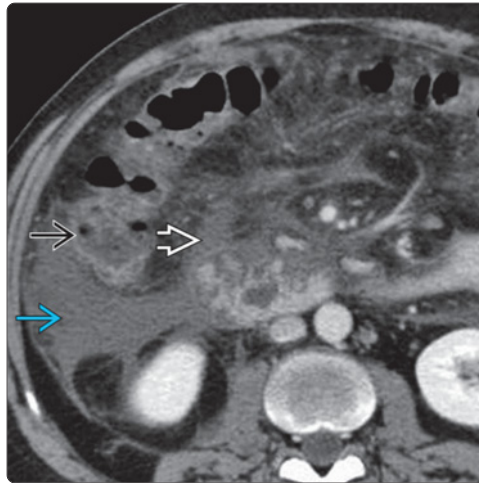
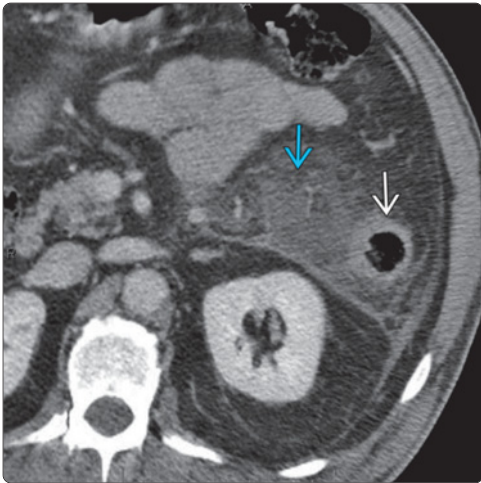
(Left) Axial CECT shows the normal anterior  & posterior  renal fascia which fuse to form the lateroconal fascia . Note that the normal fascia are extremely thin. **(Right)** Axial CECT demonstrates fluid from pancreatitis dissecting along the retromesenteric plane , formed by the layers of the anterior renal fascia and the retrorenal plane , formed by layers of the posterior pararenal space. Fluid also extends along the lateral conal fascia .



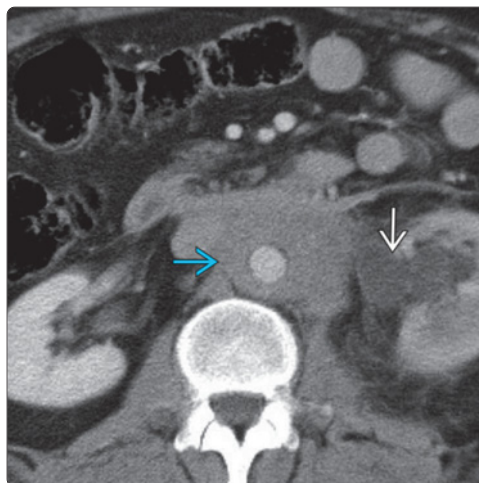
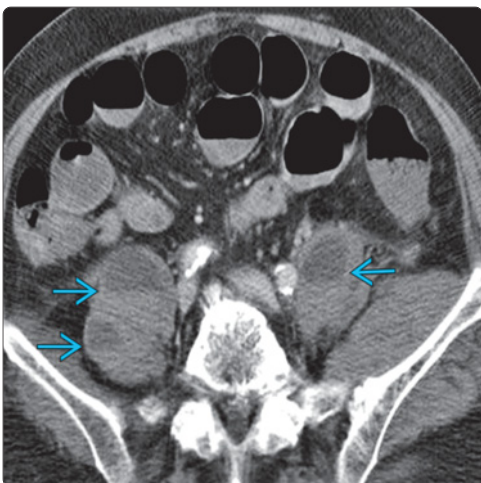
(Top) The 3 main compartments of the retroperitoneum are the anterior pararenal space (yellow), perirenal space (purple), & posterior pararenal space (blue). The interfascial planes (green) are potential spaces created by inflammatory processes that separate the double laminated layers of the renal and lateroconal fasciae. The posterior pararenal space is synonymous with the properitoneal fat that extends along the lateral & anterior abdominal wall. **(Bottom)** Sagittal graphic through the right kidney shows the 3 retroperitoneal compartments. Note the confluence of the anterior & posterior renal fasciae at about the level of the iliac crest. Caudal to this, there is only a single infrarenal retroperitoneal space.



(Left) Axial NECT in a patient following flank trauma shows that the left kidney is compressed & displaced due to a large subcapsular renal hematoma [red box]. There is also hematoma in the posterior pararenal space [red box]. Note the lack of a fluid-hematocrit level, a finding that is associated with anticoagulation hemorrhage. (Right) Axial CECT during the arterial phase reveals hemorrhage dissecting along the left interfascial planes [red box] & into the perirenal space [red box] due to contained rupture of an abdominal aortic aneurysm.



(Left) Axial CECT demonstrates fluid [red box] from subacute pancreatitis tracking into the left anterior pararenal space. Note that the descending colon [red box] also resides in the anterior pararenal space & is partially surrounded by fluid. (Right) Axial CECT demonstrates fluid from acute pancreatitis dissecting through the right aspect of the anterior pararenal space [red box]. Fluid abuts the ascending colon [red box] (also in the anterior pararenal space) & dissects along the proximal aspect of the transverse mesocolon [red box].



(Left) Axial CECT in a patient with decreased hematocrit reveals hematomas [red box] within both psoas muscles. Note the fluid-hematocrit levels within the hematomas due to anticoagulant hemorrhage. (Right) Axial CECT shows left hydronephrosis [red box] & delayed nephrogram due to obstruction of the proximal ureter. The obstruction results from retroperitoneal fibrosis (RPF) & is shown as a periaortic soft tissue mantle [red box]; unlike lymphoma, RPF does not displace the aorta from the spine.

Duplications and Anomalies of IVC

KEY FACTS

TERMINOLOGY

- Congenital anomalies of inferior vena cava (IVC)

IMAGING

- Duplication of IVC (prevalence ~ 1-3%)
 - Left- and right-sided IVC are present inferior to renal veins
 - Left IVC typically drains into left renal vein, which crosses anterior to aorta to join right IVC
 - Recognition important prior to IVC filter placement
- Left IVC (prevalence ~ 0.2-0.5%)
 - Typically drains into left renal vein, which crosses anterior to aorta to join normal right suprarenal IVC
 - Important variant in repair of abdominal aortic aneurysm and transjugular placement of IVC filter
- Azygos continuation of IVC (prevalence ~ 2-9%)
 - Absence of suprarenal IVC
 - Blood flow enters azygous vein and enters thorax posterior to diaphragmatic crus

- Enlarged azygos vein empties into SVC normally in right peribronchial location
- Hepatic veins drain directly into right atrium
- Important variant in planning cardiopulmonary bypass
- Circumaortic left renal vein (prevalence ~ 2-3.5%)
 - Important variant in nephrectomy planning
 - Rare occurrences of hematuria and hypertension

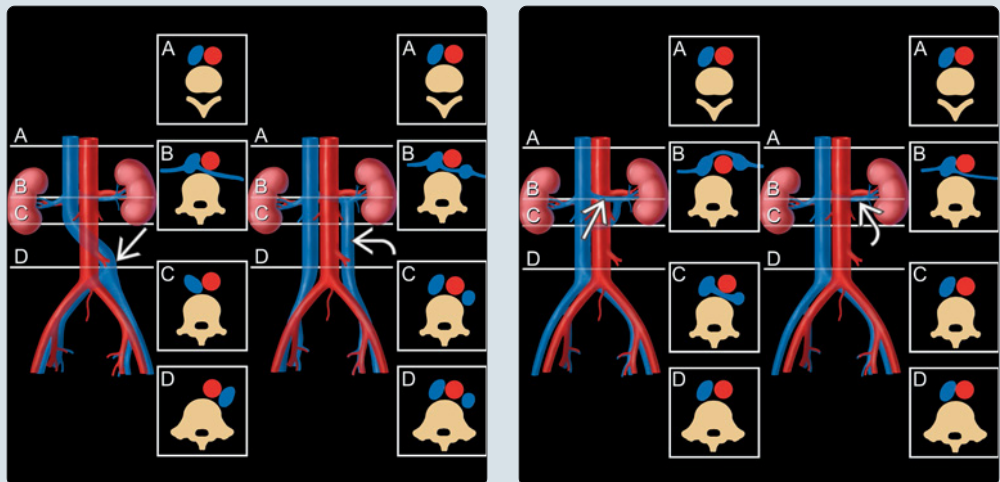
TOP DIFFERENTIAL DIAGNOSES

- Retroperitoneal lymphadenopathy
- Varices/collaterals
- Gonadal vein

DIAGNOSTIC CHECKLIST

- Preoperative imaging may be important in planning abdominal surgery, liver or kidney transplantation, or interventional vascular procedures
 - e.g., IVC filters, varicocele sclerotherapy, venous renal sampling

(Left) Graphic shows transposition of the IVC and its more common duplications. The duplicated IVC originates as the left iliac vein caudally and empties into the left renal vein. The boxes labeled "A" through "D" refer to the respective levels of the axial sections. (Right) Graphic shows a circumaortic left renal vein with a smaller ventral vein crossing cephalad to the dorsal vein.



(Left) Post-contrast axial T1 C+ FS MR with fat suppression shows a normal IVC and an additional cylindrical structure to the left of the aorta, consistent with a duplicated IVC. (Right) AP view during retrograde pyelography shows medial deviation of the right ureter due to its retrocaval course; note mild ureteral dilatation upstream from it coursing posterior to the IVC. The left ureter (not shown) had a normal course.

